Poly(lactic acid) nanoparticles and cell-penetrating peptide potentiate mRNA-based vaccine expression in dendritic cells triggering their activation

Anne-Line Coolen, Céline Lacroix, Perrine Mercier-Gouy, Emilie Delaune, Claire Monge, Jean-Yves Exposito, Bernard Verrier

Poly(lactic acid) Nanoparticles and Cell-Penetrating Peptide potentiate mRNA-based vaccine expression in Dendritic cells triggering their activation

Anne-Line Coolen, Céline Lacroix, Perrine Mercier-Gouy, Emilie Delaune, Claire Monge, Jean-Yves Exposito, Bernard Verrier

Laboratoire de Biologie Tissulaire et d'Ingénierie Thérapeutique, UMR 5305, Université Lyon 1, CNRS, IBCP – Lyon, France

Correspondence: bernard.verrier@ibcp.fr

ABSTRACT

Messenger RNA-based vaccines have the potential to trigger robust cytotoxic immune responses, which are essential for fighting cancer and infectious diseases like HIV. Dendritic Cells (DCs) are choice targets for mRNA-based vaccine strategies, as they link innate and adaptive immune responses and are major regulators of cytotoxic and humoral adaptive responses. However, efficient delivery of antigen-coding mRNAs into DC cytosol has been highly challenging. In this study, we developed an alternative to lipid-based mRNA delivery systems, using poly(lactic acid) nanoparticles (PLA-NPs) and cationic cell-penetrating peptides as mRNA condensing agent. The formulations are assembled in two steps: (1) formation of a polyplex between mRNAs and amphipathic cationic peptides (RALA, LAH4 or LAH4-L1), and (2) adsorption of polyplexes onto PLA-NPs. LAH4-L1/mRNA polyplexes and PLA-NP/LAH4-L1/mRNA nanocomplexes are taken up by DCs *via* phagocytosis and clathrin-dependent endocytosis, and induce strong protein expression in DCs *in vitro*. They modulate DC innate immune response by activating both endosome and cytosolic Pattern Recognition Receptors (PRRs), and induce markers of adaptive responses in primary human DCs *in vitro*, with prevalent Th1 signature. Thus, LAH4-L1/mRNA and PLA-NP/LAH4-L1/mRNA represent a promising platform for *ex vivo* treatment and mRNA vaccine development.

Keywords: mRNA-vaccine, nanoparticle (NP), poly(lactic acid) (PLA), LAH4-L1, Cell-Penetrating Peptide (CPPs), dendritic cells

1. Introduction

Over the past decades, traditional vaccines consisting of killed, inactivated or subunit pathogens have been successfully used against infectious diseases allowing an efficient and protective humoral immune response [1]. Despite their major successes in modern medicine, these approaches have limitations and are not applicable for chronic infections or cancers where cellular immune responses are mostly required [2]. These diseases require vaccine formulations that promote robust cell-mediated (Th1-biased) immune response instead of humoral (Th2-biased) immune response. Cellular immune responses with $CD8^+$ cytotoxic T cells (CTLs) have the unique potential to eliminate infected or altered cells, and may have a central role in host responses to viral infection like HIV and cancers [3]. CTLs are elicited against intracellular antigens produced in the cytosol, processed by the proteasome and loaded onto major histocompatibility class I (MHC-I) complexes for cell surface presentation [4]. This requires that vaccine proteins have to be delivered to the cytosol of antigenic presenting cells (APCs), like dendritic cells (DCs), which play a central function in immunity by orchestrating innate and adaptive immune responses, through antigen presentation [5].

In recent years, interest in using *in vitro* transcribed (IVT) messenger RNA (mRNA) to elicit CTLs and/or Th1-biased immune responses has exponentially increased [6–9]. mRNA vaccines have several advantages over other vaccine approaches, like a high safety profile, a flexibility to encode any protein as antigen and a simple, inexpensive and rapid production, which is of great importance in case of pandemic crisis [6,9,10]. Moreover, mRNA is transiently translated in cells and is degraded in a relatively short but controllable amount of time [7,9]. This capacity allows a more controlled antigen exposure and minimizes the risk of tolerance induction that can be associated with long-term antigen exposure [10]. One other important advantage is the higher capacity of mRNA-based vaccines to transfect non-dividing cells, as DCs, where mRNA is translated into functional protein [10]. This intracellular production of antigenic protein is responsible for antigen presentation and T-cell activation, with both $CD4^+$ and $CD8^+$ T aspects. That is why, mRNA have shown considerable promises for both prophylaxis and the treatment of various diseases, including HIV [9,11] and more than ten types of cancers [9,12].

However, to induce mRNA expression in DC, their efficient delivery into the cytosol before degradation must be achieved. In fact, exogenous mRNA must penetrate the barrier of the lipid membrane in order to reach the cytoplasm to be translated into a functional protein.

Two major strategies have been described to target DCs with mRNA [9]. The first strategy is based on *ex vivo* mRNA loading into DCs and re-infusion of the transfected cells [13]. *Ex vivo* DC loading allows an optimal control of the cellular target with high transfection efficiency. However, this is an expensive and constrained approach. The second strategy consists in a direct mRNA injection in a more rapid and cost-effective approach, but without cell type specificity. Both approaches have been explored with a variety of formulations to protect the antigenic mRNA from RNases, facilitate its uptake into cells and improve their potency [9]. Promising results have been obtained with several types of delivery system (rewiewed in [9]), including polyplexes [14–18] or lipoplexes [19–22]. But the most efficient approach currently used is based on mRNA vectorization of cationic lipid-based nanoparticles, and particularly in lipid nanoparticles (LNP) [23–27]. Some formulations have already entered clinical trials in the field of cancer immunotherapy and infectious diseases like *influenza* virus and HIV [9]. In contrast, reports on the use of polymeric nanoparticle carriers for mRNA delivery are scarce, even if they have shown great potentials in vaccination field [28–31].

Biodegradable nanoparticles based on poly(lactic acid) (PLA) backbone have gained recent interest in vaccine development. Indeed, PLA is a biodegradable and biocompatible polymer which presents a high safety profile [31] and has been approved by the Food and Drug Administration [32]. PLA-nanoparticles (PLA-NPs) constitute a versatile vectorization platform for their capacity to encapsulate and/or adsorb various antigens and immunostimulant molecules [29,30,33,34]. PLA-NPs have shown advantages in the vaccinology field for the induction of immune responses against various model antigens after parenteral administration in mammals [30,33,35]. Moreover, PLA-NPs are efficiently taken up by DCs *in vitro* and *in vivo* [33,36,37]. In fact, the nanoparticle format presents advantages for the delivery of mRNA to DCs and could improve their uptake by these cells [38]. However, both the PLA-NP surface and mRNA biomolecules are negatively charged. To adsorb mRNAs onto the surface of PLA-NPs, it is necessary to reverse the net surface charge of the NP or to design a mRNA intermediate complex which is positively charged. Thus, the use of cationic intermediates can be a promising approach. Indeed, in a pioneering work, Bettinger *et al.* demonstrated that low molecular weight cationic polymers form complexes with mRNAs [18]. Moreover, the addition of a membrane-active peptide is required for the endosomal escape of these complexes, and efficient mRNA translation in the cytosol. Recent studies have proposed that cationic cell-penetrating peptides (CPPs), small peptides composed of 8 to 30 amino acids with a net positive charge, might constitute an excellent vehicle for

mRNA delivery [39]. They combine low charge densities with an ability to induce membrane disruption for endosomal escape. In fact, this process is essential to allow cytosol delivery of mRNA where it can be recognized by protein synthesis apparatus and translated into protein [10].

In this study, we have developed and compared new mRNA platforms using three different CPPs (RALA, LAH4 and LAH4-L1) as cationic intermediates for vectoring mRNA onto PLA-NPs. We have evaluated the interest of these peptide/mRNA polyplexes and PLA-NP/peptide/mRNA nanocomplexes to transfect DCs and activate innate and immune signaling responses through transcriptomic analysis. The highest protein expression in DCs was observed with LAH4-L1 and PLA-NP/LAH4-L1 formulations. These formulations trigger innate immunity through PRR activation and activate adaptive immune responses, including a prevalent Th1 aspect. To understand the mechanisms of each formulation involved in these *in vitro* activations, we also have investigated the uptake mechanism and the intracellular traffic of particles in DCs, indicating a clathrin-mediated endocytosis and phagocytosis pathways. Thus, these data show that LAH4-L1/mRNA polyplexes and PLA-NP/LAH4-L1/mRNA nanocomplexes are promising platforms for mRNA vaccine delivery to DCs.

2. Materials and methods

a. Production of in vitro transcribed mRNA

pGEM4z-HxB2gag-64A encoding Gag antigen was kindly given by Guido Vanham (University of Antwerp, Antwerp, Belgium). The HxB2 gag gene is under the control of a T7 promoter and a unique *Ehe*I restriction site is located just downstream of the $(A)_{64}$ tail. pGEM4z-HxB2gag-64A was propagated in NEB® Stable *Escherichia coli* bacteria (New England Biolabs (NEB), France) and purified using NucleoBond Xtra Maxi Endotoxin Free kit (Macherey-Nagel, France). The plasmid was linearized with *Ehe*I restriction enzyme (NEB), purified using a Wizard Genomic DNA Purification Kit (Promega, France), and used as a DNA template for *in vitro* transcription. Capped mRNA transcripts (IVT) were produced using the T7 MessageMachine Kit (Ambion, Life technologies, France). mRNA purification was performed by DNase I digestion, followed by LiCl precipitation and mRNA pellet was solubilized in RNase-free water.

eGFP mRNA encoding green fluorescent protein was provided by Guido Vanham (University of Antwerp, Antwerp, Belgium). RNA was quantified by spectrophotometric

analysis at 260 nm and analyzed by standard agarose gel electrophoresis to confirm the integrity of this full-length mRNA. All mRNAs were stored in RNase free water at −80 °C.

b. Production of fluorescent labeled mRNA

Gag mRNA was labeled with MF488 using the Label IT Nucleic Acid Labeling Reagent kit (Mirus, Euromedex, France) according to the manufacturer's instructions. Briefly, 5 µg of mRNA was stained with kit reagents for 1 h at 37°C, and fluorescent mRNA was purified using ethanol precipitation. The pellet was resuspended with 10 µL of nuclease-free water and mRNA labeled was quantified by spectrophotometric analysis, while mRNA integrity was checked through agarose gel electrophoresis.

c. Polyplexes and nanocomplexes preparation and characterization

To form polyplex, mRNA was diluted in RNA-free water at 40 ng/µL and mixed (V/V) with 800 ng/µL in RNA-free water of LAH4-L1 (KKALLAHALHLLALLALHLAHALKKA), LAH4 (KKALLALALHHLAHLALHLALALKKA) or RALA (WEARLARALARALARHLARALARALRACEA) peptides (GeneScript, China). Then, equal volumes of those polyplexes and PLA-NP (at 0.5% in water; Adjuvatis, France) were mixed to form PLA-NP/Peptide/mRNA nanocomplexes.

The hydrodynamic diameter and zeta potential (surface charge) of mRNA formulations were determined by dynamic light scattering (DLS) using the Zetasizer Nano ZS (Malvern Instrument, U.K.).

Complexes were also analyzed using an electrophoretic mobility shift assay (ESMA). In some samples, a heparin/proteinase K treatment was performed in order to separate mRNA from the complexes. Briefly, complexes were first treated or not with heparin (Sigma, France) during 1 h at RT, and secondly with proteinase K (NEB, France) at 56°C during 30 min. Each sample (treated or not) containing 200 ng mRNA was loaded into one well and analyzed by electrophoresis in a standard 1% agarose gel in presence of ethidium bromide (Genesee Scientific).

To highlight the association between mRNA and PLA-NP, a Fluorescence Resonance Energy Transfer (FRET) assay was performed. Components were associated as described above, with a Ribogreen fluorescent mRNA (Quant-IT Ribogreen™ RNA assay kit, Invitrogen) and CellTrace™ BODIPY-TR Methyl Ester fluorescent PLA-NP (Adjuvatis, France). 100 µL of each complex was deposited in triplicate in black 96-plate well (flat-bottom). Fluorescence was recorded on Tecan i-control Infinite M1000) (Tecan, Swiss) for

Ribogreen™ (460nm/520nm), BODIPY-TR (561nm/625nm) and FRET (460nm/625nm). Fluorescence was determined as the mean of three independent experiments and results were normalized to remove the contribution of free PLA-NPs.

d. Expression efficiency analysis

Immortalized DC2.4 (a murine bone marrow derived dendritic cell lines [40] and kindly provided by Jacqueline Marvel group (CIRI, France)) was propagated in complete RPMI-1640 medium with 10 % heat-inactivated fetal bovine serum (FBS), 10 mM Hepes and 50 µM β-mercaptoethanol (Gibco, Life Technologies, France) at 37° and 5 % CO_2. HeLa (ATCC® CCL-2™) and HEK293(ATCC® CRL-1573™) were cultured in DMEM containing 10% heat-inactivated FBS (Gibco, Life Technologies, France) at 37°C and 5 % CO2. Cells were used with a low passage number (less than 12).

One day before transfection, cells were seeded in a 96-well plate at the density of 25 000 cells (in 100 µL of complete medium) per well. After 24 h, complete medium was replaced by 100 µL of serum-free medium. Formulations were added to cells with a volume allowing the transfection of 20 ng of eGFP mRNA or equivalent volume for controls. Four hours after transfection, supernatants were removed and 100 µL of complete medium was added. Then, cells were incubated at 37°C and 5% CO2 until the analysis (0 to 48 h). Positive control of transfection was performed with Trans IT®-mRNA Transfection Kit (Mirus, Euromedex, France) using the manufacturer's recommendations. Briefly, 0.5 µg of mRNA was added to 50 µL of serum-free medium, and 1 µL of Trans IT mRNA reagent and 1 µL of mRNA Boost Reagent were then added. After 5 min at room temperature, complex mixture was added to cell at the desired concentration. Negative controls were performed with peptide alone, PLA-NP/Peptide complex, naked PLA-NP and naked mRNA at equivalent concentrations that nanocomplexes.

To quantify the percentage of eGFP fluorescent-positive cells and Mean Fluorescence Intensity (MFI), transfected DCs were harvested, stained with propidium iodide (Invitrogen) and analyzed by AccuriC6 flow cytometer (BD Biosciences) on the platform "AniRA cytométrie" (SFR BioSciences, UMS3444/CNRS). Dead cells were excluded using propidium iodide, and then living DCs were gated based on their large forward scatter (FSC) and large side scatter (SSC) profile, to avoid cell debris. Data analysis was performed with BD Accuri C6 Software CFlow Plus (BD Biosciences). Data were determined as the mean of three independent experiments.

e. Stability of formulations

To verify formulation stability, polyplexes and nanocomplexes were prepared and conserved at 4°C during 21 days. At each time-point, the hydrodynamic diameter and zeta potential were determined by DLS using the Zetasizer Nano ZS (Malvern Instrument, U.K.) and the expression efficiency was determined as described in the precedent part by flow cytometry.

f. Cytotoxicity of formulations

Cytotoxicity of complexes was evaluated by Presto Blue Assay (Thermo Fisher Scientifc) according to the manufacturer's instructions. Briefly, DC2.4 cells were seeded at a density of 25 000 cells/well into 96-well plates a day prior to the transfection. Transfection with complexes was performed, as previously described, with a volume allowing the transfection of 20 ng of eGFP mRNA or equivalent volume for controls, and cytotoxicity was measured 24 h later. After incubation, 10 µL of Presto Blue Reagent was added and plates were incubated 10 min at 37°C. Fluorescence was detected on Tecan i-control Infinite M1000 (560nm/590nm; Bandwidth 10 nm; Gain 91) (Tecan, Swiss). Fluorescence was determined as the mean of two replicates and three independent experiments.

g. Endocytosis mechanisms analysis

DC2.4 cells were seeded into 96-well plates at the density of 25000 cells/well a day prior to the transfection. Medium was removed 15 min before transfection and 100 µL of serum-free medium in presence of one molecule inhibitor was added. Used concentrations and mode of action of genistein, chlorpromazine, dynasore, nocodazole, amiloride, pimozide and cytochalasine inhibitors were indicated in supplementary data (**Table I)**. After 15 min, cells were treated with formulations (with a volume allowing the transfection of 20 ng of eGFP mRNA or equivalent volume for controls) during 2 h. To analyze uptake efficiency, cells were incubated with an MFP488 fluorescent mRNA alone or in complex. After 2 h, cells were harvested, treated with 0.2% trypan blue and analyzed by flow cytometry, as described previously.

h. Endosome escape evaluation

DC2.4 were seeded into 96-well plates at the density of 25000 cells/well a day prior to the transfection. Cells were treated 15 min before transfection with 175 mM of Bafilomycine A1 (Invivogen, France) in 100 µL of serum-free media. Complexes and associate controls were added (with a volume allowing the transfection of 20 ng of eGFP mRNA or equivalent

volume for controls) for 4 h. After medium replacement, cells were incubated 12 h at 37°C and 5% CO2, and then they were harvested and analyzed by flow cytometry as described previously.

i. Immunostainning of moDCs

To verify gag expression in moDCs, p17 protein (a component of gag polyprotein) was stained in moDCs. Cells were seeded at a seeding density of 50 000 cells/well into µSlide 12 well Chamber (Ibidi, Germany) and transfected as previously described with a volume allowing the transfection of 40 ng of mRNA or equivalent volume for controls in 200 µL of serum-free medium for 2 h. Then, cells were rinsed with PBS 1X, fixed with 4% paraformaldehyde for 20 min at RT, permeabilized in 0.1% Triton-PBS 1X at RT for 15 min and saturated with 1% BSA-PBS 1X for 1 h at RT. After saturation, cells were incubated 2 h with anti-p17 (5 µg/mL; kindly given by Christophe Guillon, CNRS/University of Lyon, France), washed and stained with secondary antibody FITC anti Mouse IgG (5 µg/mL; Jackson Immuno Research) in the dark for 1 h at RT. Then, cells were washed and mounted on glass slides using Vectashield mounting medium with DAPI (Vector laboratories). Slides were analyzed using a SP5 upward confocal microscope (Leica) with 63×/1.4NA objective and data were analyzed using ImageJ Software.

j. Determination of innate immune-stimulatory activity

HEK-Blue hTLR7 and HEK-Blue hTLR73 reporter cell lines (InvivoGen) were used as specified by the manufacturer to detect TLR7 and TLR3 stimulation. Briefly, 50 000 cells/well were seeded into 96-well plates and stimulated during 24 h with the different formulations. TLR7 or TLR3 activation was monitored by quantifying the amount of the secreted embryonic alkaline phosphatase (SEAP) which is placed under the control of IFN-β minimal promoter fused to five NF-κB and AP-1-binding sites. The level of alkaline phosphatase can be determined with a detection medium that turns blue in its presence. Sample absorbance was measured at 620 nm using a microplate reader (Bio-Rad).

k. Preparation and stimulation of human monocyte-derived DCs

Monocytes were purified from human peripheral blood and differentiated into moDCs as previously described [33]. Briefly, PBMCs were isolated from venous blood samples (from Etablissement Français du Sang, Lyon) by density gradient centrifugations using Ficoll-Paque™ plus and Percoll (GE Healthcare). Remaining erythrocytes, NK, B- and T- cells were then depleted by anti-glycophorin A, anti-CD56, anti-CD19 and anti-CD3 antibodies

(Beckman Coulter) respectively, using Dynabeads® Pan Goat antimouse IgG (Invitrogen). To differentiate purified monocytes (0.5×10^6 cell/ml) into MoDCs, cells were cultured in RPMI medium supplemented with 10% heat-inactivated fetal bovine serum (FBS), gentamycin (50 U/ml), 100 U/ml penicillin and 100 μg/ml streptomycin in the presence of 62.5 ng/ml of human interleukin-4 (IL-4) (Miltenyi Biotec, France) and 75 ng/ml of human granulocyte macrophage colony stimulating factor (GM-CSF) (Miltenyi Biotec, France). After 6 days, complexes were added to 1×10^6 differentiated moDCs in similar culture medium depleted of serum for 2 h (volume allowing the transfection of 660 ng of gag mRNA or equivalent volume for controls). After addition of FCS, cells were incubated 24 h or 48 h at 37 °C, 5% CO2. DCs only cultured in complete RPMI medium were used as a negative control of stimulation, and those cultured in the presence of 2.5 μg/ml of LPS (Invivogen, France) were used as a positive control.

DC maturation was assessed by cell surface immunostaining using monoclonal antibodies against lineage markers and co-stimulatory molecules. Cells were then stained with anti–CD1a-FITC, anti-CD14-FITC, anti-HLA DR-FITC, anti HLA-ABC-FITC, anti-CD40-PE, anti-CD80-PE, and anti–CD86-PE mAbs (BD Pharmingen). Data were acquired using a FACSCanto flow cytometer (BD Biosciences) and analyzed with FlowJo software (Tree Star).

l. Real-time qPCR analyses

The different complexes were incubated 2 h to 4×10^6 of differentiated moDCs without serum (volume allowing the transfection of 2640 ng of gag mRNA or equivalent volume for controls). FBS was added and cells were incubated at 37 °C, 5% CO2. After 6h of incubation, RNA was extracted from moDCs using QIamp RNA Blood Mini Kit (Qiagen). Using 0.5 ng of mRNA per conditions, the expression of 84 genes was quantified using an RT^2 Profiler PCR Array Human Innate and Adaptive Immune Response plate (PAHS-052Z, Qiagen). Data were acquired using a AriaMx Real-time PCR System (Agilent) and analyzed with GeneGlobe Data Analysis Center (Qiagen).

m. Quantification of cytokines

The experimental procedure is similar to the one used for moDC stimulation. After stimulation by complexes during 24 h and 48 h, supernatant was harvested and cytokine and chemokine quantifications were performed using a Luminex Magpix instrument (Bio-Rad) in combination with human Miliplex cytokine/chemokine immunoassay kit (HCYTMAG-60K-PX29, Merck). Data were analyzed with BioPlex Manager (BioRad). For each condition,

concentrations were determined as the mean of three replicates for each independent experiment (N=3). We excluded from the standard curve any points with accuracy outside of 70-130 %. The coefficient of variation of the three assayed were shown to be less than 20% CV for all data.

n. Statistical Analysis

Statistical analysis was performed using GraphPad Prism Version 6.0 software. All of the data are presented as the mean ± SEM. Difference between groups was analyzed as described in figure legends. Statistical significances were indicated on the figures.

3. Results:

a. mRNAs can be associated onto PLA-NPs via cationic peptides

In order to vectorize mRNAs, we designed novel formulations based on polymeric nanoparticles, PLA-NPs, which have demonstrated several advantages in the vaccination field. Whereas hydrophobic molecules can be efficiently encapsulated in the core of PLA-NPs, the hydrophilic nature of mRNAs prevents their simple encapsulation into PLA-NPs. Instead, we developed strategies to adsorb mRNAs at the surface of PLA-NPs. Because the PLA-NP surface and mRNAs are both negatively charged, we used cationic peptides as an intermediate between mRNA and PLA-NPs. We compared three positively charged cell-penetrating peptides (CPPs) with nucleic acid condensation properties: RALA, LAH4 and LAH4-L1. Those cationic peptides are predicted to have a helical structure with amphipathic profile, which presents advantages for cellular uptake and membrane disruption (**Fig. S1**). In this strategy, mRNAs were first complexed with cationic peptides to form polyplexes, which were subsequently adsorbed onto PLA-NPs to produce nanocomplexes, as described in Materials and Methods section (**Fig. 1A**). The PLA-NP doses used in the formulations were shown to be non-toxic in a previous work from our laboratory [41].

The hydrodynamic diameter and zeta potential of nanocomplexes formed with the 3 cationic peptides were analyzed by DLS (**Fig. 1B**). The addition of Peptide/mRNA polyplexes onto PLA-NPs (~ 188 nm; -50 mV) induced an increase in size and an inversion of the surface charge, as reflected by the zeta potential of ~ 30mV, suggesting that the 3 types of polyplexes are efficiently adsorbed onto PLA-NPs. The LAH4 peptide induced the formation of larger nanocomplexes (~ 275.8 nm) than RALA and LAH4-L1 (~ 237.8 nm and ~ 220.1 nm, respectively) with the highest polydispersity index (PdI). For RALA and LAH4-L1 peptides, the polydispersity indexes in the final formulations were close to 0.1 (PdI=0.134 and 0.129,

respectively), reflecting that the nanocomplexes were homogenous in size. As shown for LAH4-L1 in Fig. S2, the pre-formulation peptide/mRNA polyplexes presented a high polydispersity index (PdI=0.3), the size distribution graph indicating the presence of aggregates. Yet, the addition of PLA-NP, which are highly monodisperse and negatively charged, allowed a modification of the equilibrium of charges to form a monodisperse final product (PdI=0.129) with a rearrangement of peptide/mRNA polyplexes at the surface of PLA-NP. Finally, we showed that the colloidal formulations were stable for 14 days at 4°C, as indicated by hydrodynamic diameter and zeta potential measurements (results obtained with LAH4-L1 peptide are shown in **Fig. S3**).

To verify the ability of peptides and PLA-NPs to bind mRNAs, an electrophoretic mobility shift assay (EMSA) was applied (**Fig. 1C**). To detach mRNA from the complexes, a treatment with heparin (for PLA-NP detachment) and proteinase K (for peptide degradation) was performed. The same results were obtained for RALA, LAH4 and LAH4-L1 peptides: mRNA complexed with one of these peptides or in PLA-NP nanocomplexes were retained in the wells, while their electrophoretic mobility was identical to that of naked mRNA after heparin/proteinase K treatment. To confirm the binding of Peptide/mRNA polyplexes onto the surface of PLA-NPs, another test based on Fluorescence Resonance Energy Transfer (FRET) was developed. In this test, we used red fluorescent PLA-NPs (containing BODIPY-TR Methyl Ester dye) and a green fluorescent mRNA (labelled with Ribogreen^{TM}). The close proximity of green fluorescent mRNAs to red fluorescent PLA-NPs causes red fluorescence emission (625 nm) upon Ribogreen^{TM} excitation (460 nm). PLA-NP/LAH4-L1/mRNA nanocomplexes displayed significantly higher 625 nm emission than that obtained in samples containing a simple mix of mRNAs and PLA-NPs (**Fig. 1D)**, confirming the presence of mRNA nearby the core of PLA particles (distance < 10 nm).

Altogether, these results confirm the ability to form stable nanocomplexes of mRNAs and PLA-NPs using RALA, LAH4 or LAH4-L1 peptides. mRNA condensation capacity of CPPs was conserved after polyplex adsorption onto PLA-NP.

A

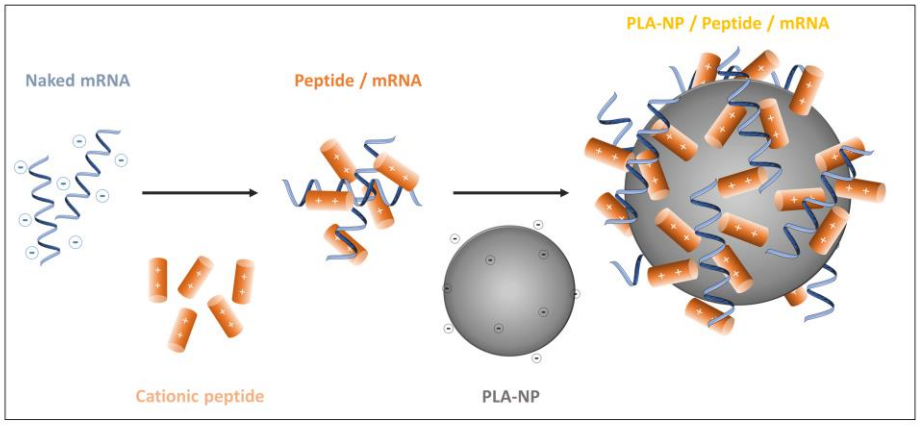

B

Nanocomplex	Hydrodynamic diameter (nm)	PdI	Zeta potential (mV)
PLA-NP	188.0 (± 1.80)	0.053 (± 0.046)	- 51.8 (± 0.6)
PLA-NP / **RALA** / mRNA	237.8 (± 29.2)	0.134 (± 0.0.57)	+ 34.8 (± 5.2)
PLA-NP / **LAH4** / mRNA	275.8 (± 43.2)	0.244 (± 0.051)	+ 29.0 (± 4.4)
PLA-NP / **LAH4-L1** / mRNA	220.1 (± 22.9)	0.129 (± 0.058)	+ 37.3 (± 4.4)

C

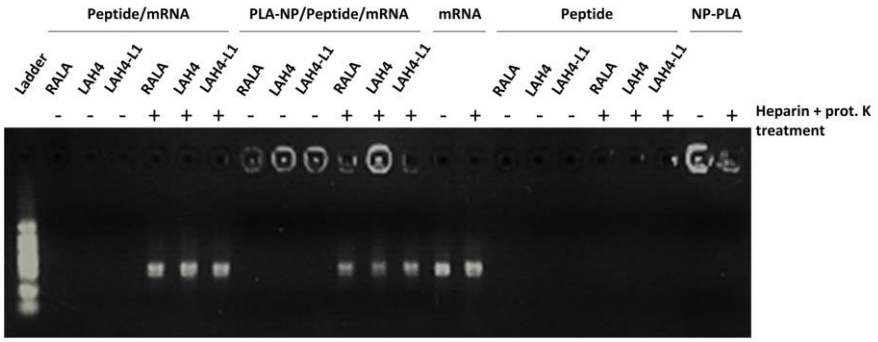

D

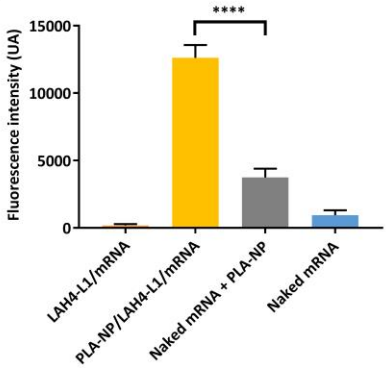

Fig 1. mRNA can be vectorized by PLA-NPs using cationic peptides as intermediates. *(**A**) Schematic representation of the vectorization strategy of mRNAs onto PLA-NPs. Negatively charged mRNA was associated with cationic peptides (RALA, LAH4 or LAH4-L1) to form Peptide/mRNA polyplexes. Then, this complex was adsorbed onto PLA-NPs to form PLA-NP/Peptide/mRNA nanocomplexes. (**B**) Comparison of thermodynamic diameter, polydispersity index (PdI) and zeta potential of nanocomplexes formed between the 3 peptide/mRNA combinations and naked PLA-NPs. Each value provided is the average of four series of measurements and four independent experiments (N=4). (**C**) Electrophoretic mobility shift assay showing eGFP mRNAs complexed with peptides or in PLA-NP/Peptide/mRNA nanocomplexes. A heparin and proteinase K (prot. K) treatment (+) was applied to the samples in order to detach the mRNA from the complexes. (**D**) Fluorescence Resonance Energy Transfer (FRET) analysis. Red fluorescence emitted by different formulations was evaluated after green fluorescent mRNA (RiboGreen) excitation (n=3). Statistical significance between two groups was determined using a one-way Anova: *, $p < 0.05$; **, $p < 0.01$; ***, $p < 0.001$; ****, $p < 0.0001$.*

b. LAH4-L1-based formulations allow efficient mRNA uptake and protein expression in dendritic cells

The ability of mRNA complexes to transfect DCs was evaluated *in vitro* using the mouse DC2.4 cell line as a model (**Fig. 2A-C**). To that end, each complex containing an equivalent of 20 ng of eGFP mRNA was added to DC2.4 cells in serum-free conditions, and the percentage of GFP positive cells (**A-B-C**) and the Mean Fluorescence Intensity (MFI) (**A'-B'-C'**) were measured after 16h by flow cytometry. As a control, the same amount of naked eGFP mRNA was transfected into DC2.4 cells using the commercial TransIT-mRNA transfection kit (Mirus Bio). As shown in **Fig. 2A-A'**, mRNA complexes formed with RALA peptides failed to efficiently transfect DCs, while a low transfection capacity was observed in LAH4 peptide assays (**Fig. 2B-B'**). However, LAH4-L1-based formulations induced an efficient transfection of DC2.4. With LAH4-L1/mRNA polyplexes or PLA-NP/LAH4-L1/mRNA nanocomplexes, about 35% or 57% of DC2.4 cells expressed eGFP mRNA, respectively, with a significantly higher transfection efficiency than TransIT control assay (**Fig. 2C**). Moreover, the intensity of expression was significantly more important using PLA-NP/LAH4-L1/mRNA nanocomplexes than TransIT or LAH4-L1/mRNA assays (p-value < 0.05) (**Fig. 2C'**). These results indicate that transfection efficiency is potentiated by the presence of PLA-NPs in the formulations.

A time-course study of eGFP expression in DCs was performed to compare mRNA/LAH4-L1 polyplexes and PLA-NP/LAH4-L1/mRNA nanocomplexes. At 4 h post transfection, eGFP-expressing DCs were already detectable, and the number of positive cells reached a plateau in all assays at 16-24 h post transfection (**Fig. 2D**). Interestingly, a bi-phasic curve was observed for the intensity of fluorescence, with a rapid increase until 16 h and a gradual decrease after 24 h (**Fig. 2D'**). The amount of GFP positive cells and the MFI were higher with PLA-NP/LAH4-L1/mRNA than with LAH4-L1/mRNA or TransIT-mRNA complexes, up to 48 h post transfection (**Fig. 2D-D', Fig. S4**). These nanocomplexes showed stable expression efficiency after storage at 4°C for up to 7 days (results obtained with LAH4-L1 peptide were shown in **Fig. S4**). We did not observe any toxicity of the formulations in DCs under the conditions of the experiments (**Fig. 2E**).

The uptake of LAH4-L1-based formulations by different cell types was investigated. LAH4-L1 polyplexes and nanocomplexes failed to transfect HEK293 and HeLa cells, two epithelial cell lines, in the same experimental conditions (**Fig. 2F-G**). These results indicate

that the transfection capacity of LAH4-L1/mRNA and PLA-NP/LAH4-L1/mRNA complexes depends on cell type and seem to be particularly efficient to target DCs.

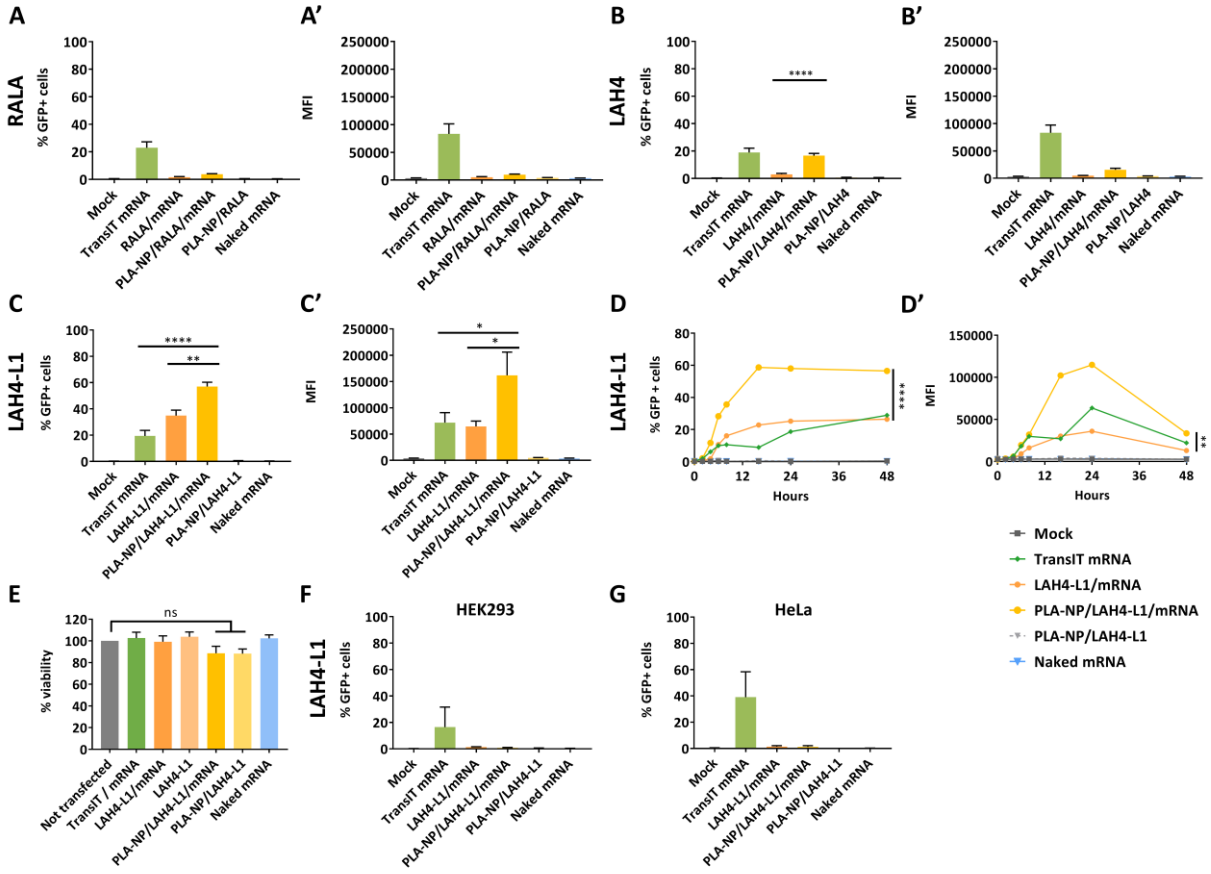

Thus, LAH4-L1/mRNA and PLA-NP/LAH4-L1/mRNA formulations constitute efficient methods for DC transfection with low doses of mRNA. We focused on these two formulations for further analysis.

Fig. 2. LAH4-L1-based formulations allow efficient mRNA expression in DC2.4 cells in vitro. *Untreated DCs (Mock), TransIT eGFP mRNA (positive control), eGFP mRNA complexes and negative controls (PLA-NP/LAH4-L1 and naked mRNA) were transfected in serum-free medium for 4 h (20 ng mRNA/well). The transfection efficiency was measured 16h after the addition of mRNA complexes to the cells. (**A-C'**) Percentage of green fluorescent protein (eGFP) positive DC2.4 cells (A-B-C) and mean fluorescence intensity (MFI) (A'-B'-C') were quantified after transfection in presence of RALA-, LAH4- and LAH4-L1-based complexes (n=3). (**D-D'**) Kinetics of expression efficiency after transfection with LAH4-L1-based formulations. The percentage of eGFP positive DC2.4 cells (D) and the MFI (D') are presented. (**E**) Cytotoxicity of LAH4-L1-based nanocomplexes on DC2.4 cells. (**F-G**) Percentage of eGFP positive DC2.4 cells after LAH4-L1-based formulations transfections in (**F**) HEK293 and in (**G**) HeLa cells (n=3). Statistical significance of differences between two groups was determined using one-way or two-way Anova: *, $p < 0.05$; **, $p < 0.01$; ***, $p < 0.001$; ****, $p < 0.0001$.*

c. mRNA vaccine formulations enter in dendritic cells through clathrin-mediated endocytosis and phagocytosis

To understand the intracellular mechanisms allowing mRNA expression, we monitored the cellular uptake of LAH4-L1-based formulations by DCs. We studied their

mechanisms of internalization by treating DC2.4 cells with various endocytosis inhibitors. Targets and action mechanisms of each inhibitor were described in supplementary **Table I**. To visualize the complexes, we used MFP488-labelled fluorescent mRNAs. The mRNAs were complexed with LAH4-L1 or PLA-NP/LAH4-L1 and incubated for 2 h with inhibitor treated DC2.4 cells. To distinguish between complexes located inside the cells or at cell surface, extracellular fluorescence was quenched with trypan blue [42]. The percentage of cells taking up MFP488 mRNAs and the MFI were measured by flow cytometry (**Fig. 3A-B**). Surprisingly, the same profiles were obtained for LAH4-L1/mRNA polyplexes and PLA-NP/LAH4-L1/mRNA nanocomplexes. Aggregation presence with LAH4-L1/mRNA polyplexes can explained this result. Cells treated with chlorpromazine or dynasore, two clathrin-mediated endocytosis inhibitors, and with pimozide, a phagocytosis inhibitor, showed a significant decrease of MFP488 fluorescence (p-value < 0.0001). In agreement with a role of the clathrin-dependent and phagocytosis pathways, inhibition of microtubule and actin polymerization with nocodazole and cytochalasin D, respectively, also induced an important decrease of complexes uptake by DCs.

These results suggest that clathrin-dependent endocytosis and phagocytosis are important mechanisms involved in the uptake of LAH4-L1/mRNA polyplexes and PLA-NP/LAH4-L1/mRNA nanocomplexes by DCs. On the contrary, the lack of inhibition by genistein and amiloride suggests that caveolae-dependent endocytosis and macropinocytosis are not essential for this uptake.

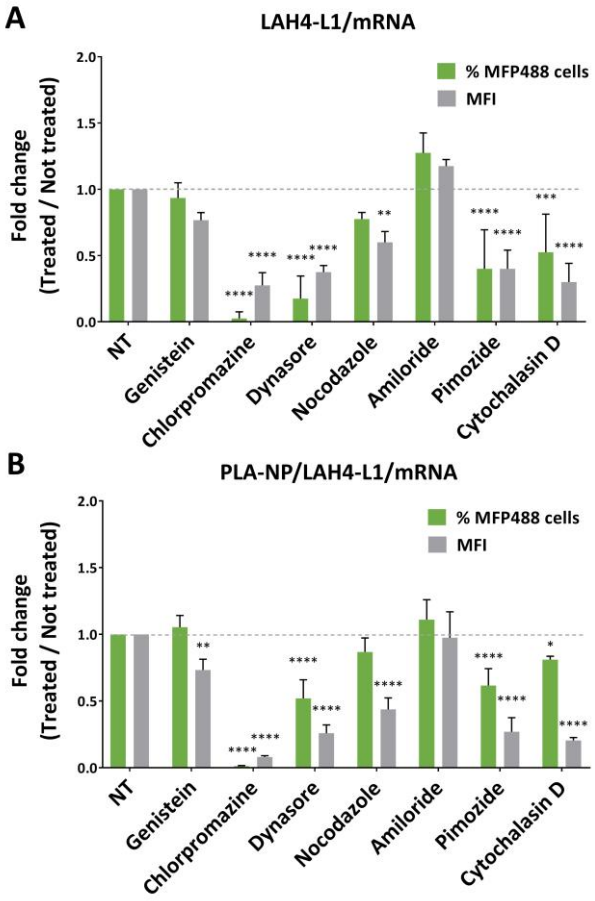

Fig 3. Clathrin-mediated endocytosis and phagocytosis are involved in complexes uptake by DC2.4 cells. *Uptake efficiency of MFP488-labelled mRNA complexed with LAH4-L1 (**A**) or PLA-NP/LAH4-L1 (**B**). MFP488 mRNA was incubated for 2 h with DC2.4 cells in presence of various inhibitors, and uptake efficiency was quantified by flow cytometry (n=3). Green bars: percentage of cells which present intracellular MFP488 fluorescence; White bars: Mean of fluorescence (MFI). Green bars: percentage of GFP positive cells; Grey bars: MFI. The value of not treated cells (NT) were set as 1. Statistical significance between two groups was determined using a two-way Anova test: *, $p < 0.05$; **, $p < 0.01$; ***, $p < 0.001$; ****, $p < 0.0001$.*

d. Endosomal escape is needed to induce efficient translation

The previous results suggest that clathrin-mediated endocytosis and phagocytosis are involved in the cellular uptake of formulations. These pathways induce the formation of vesicular structures that eventually fuse with lysosomes. To allow mRNA expression, nanocomplexes must escape the endosomes before lysosome fusion. Positive charges of amphipathic cationic LAH4-L1 have been involved in this endosomal escape through the proton sponge effect [43]. To evaluate the importance of this proton sponge mechanism, we performed a transfection in presence of Bafilomycin A1, a specific inhibitor of vacuolar proton ATPases, which is essential for proton regulation in endosome. The percentage of eGFP positive cells and the MFI were measured after 16 h by flow cytometry (**Fig. 4**). In presence of Bafilomycin A1, the percentage of eGFP positive cells and the MFI were drastically reduced.

These results show the importance of endosome acidification for eGFP mRNA expression, in agreement with a model whereby a proton sponge effect allows mRNA escape from the endosomes to the cytosol.

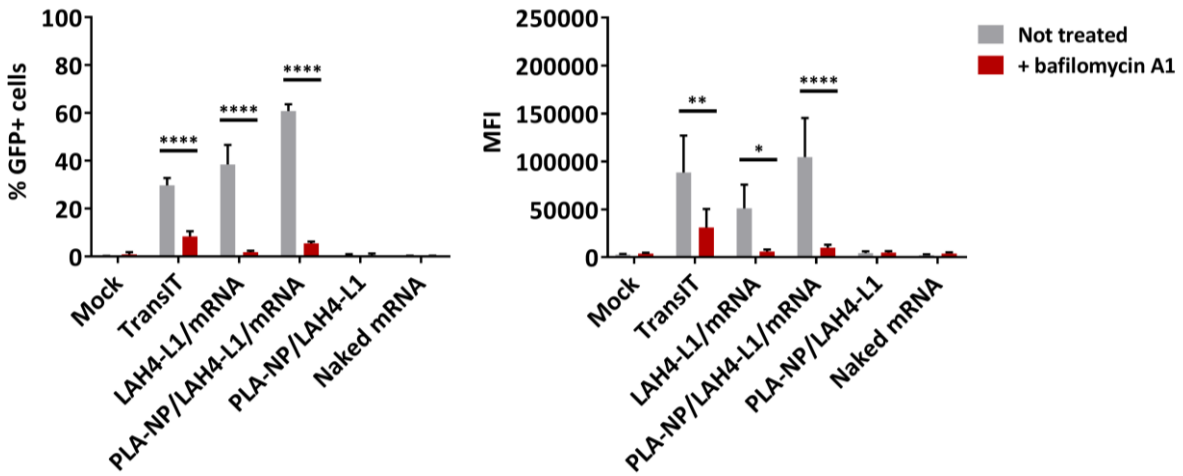

Fig 4. Endosomal escape is essential for mRNA expression in DC2.4 cells. *Percentage of eGFP positive DC2.4 cells and mean fluorescence intensity (MFI) were quantified after 16 h of transfection by LAH4-L1-based formulations in absence (grey bars) or in presence (red bars) of bafilomycin A1 (n=3). Statistical significance between two groups was determined using a two-way Anova test: *, p < 0.05; **, p < 0.01; ***, p < 0.001; ****, p < 0.0001.*

e. mRNAs in LAH4-L1-based formulations induce an innate immune-stimulatory activity through PRR activation

We then analyzed the immune-stimulatory properties of LAH4-L1-based formulations, using mRNAs coding for the Gag protein of HIV-1, a model antigen protein relevant for vaccine development. DCs express a repertoire of PRRs allowing the recognition of a large range of pathogen molecules, including some RNA sequences. The intrinsic adjuvant activity of formulations was evaluated *in vitro* using cell lines which overexpress only one specific PRR (h-TLR7 or h-TLR3). These cell lines were transfected with different nanocomplex concentrations and PRR activation was evaluated (**Fig. 5A-B**). LAH4-L1/mRNA and PLA-NP/LAH4-L1/mRNA complexes induced a significant h-TLR3 activation in a dose-dependent manner, while the same complexes devoid of gag mRNA only activated weakly h-TLR3 cells while a non-significant h-TLR7 activation was observed. These results show the specific TLR3 immune-stimulation activity of PLA-NP/LAH4-L1/mRNA nanocomplexes. In this experiment, the mRNA complexed onto LAH4-L1-based formulations seemed to be taken up by modified HEK293 cell lines to activate endosomal PRR, whereas **Fig. 2F** showed that mRNAs are not translated into functional protein in HEK293. Those observations suggest an alteration of RNA escape from endosome or of translation in this cell type.

To further analyze the immune-stimulatory properties of LAH4-L1-based formulations, subsequent experiments were performed using primary DCs derived from human monocytes (moDCs), a cellular model particularly suitable for activation studies. A comparative gene expression analysis was carried out on moDCs treated with the different formulations, using the Human Innate and Adaptive Immune Responses RT2 Profiler™ PCR Array. After 6 h of stimulation, the formulations induced a modification in the expression pattern of multiple genes encoding TLR and signaling proteins associated to their pathways (**Fig. 5C**). Main effects were observed for formulations containing the LAH4-L1 peptide. PLA-NPs and mRNAs alone did not have the ability to modify the gene expression profile. However, the presence of mRNA in formulations (see LAH4-L1/mRNA vs LAH4-L1 and PLA-NP/LAH4-L1/mRNA vs PLA-NP/LAH4-L1) upregulated the expression of TLR3, TLR7 and DDX58 (also called RIG-I), three PRR receptors involved in RNA recognition [44]. Their target genes (IRFF7, MYD88, NFKB1, and TICAM1) were also upregulated after LAH4-L1/mRNA stimulation. Interestingly, these formulations decreased the expression of other TLR genes, suggesting that the presence of mRNAs favors a signaling through

TLR3/TLR7/DDX58. However, it should be noted that the data shown in **Fig.5C** only

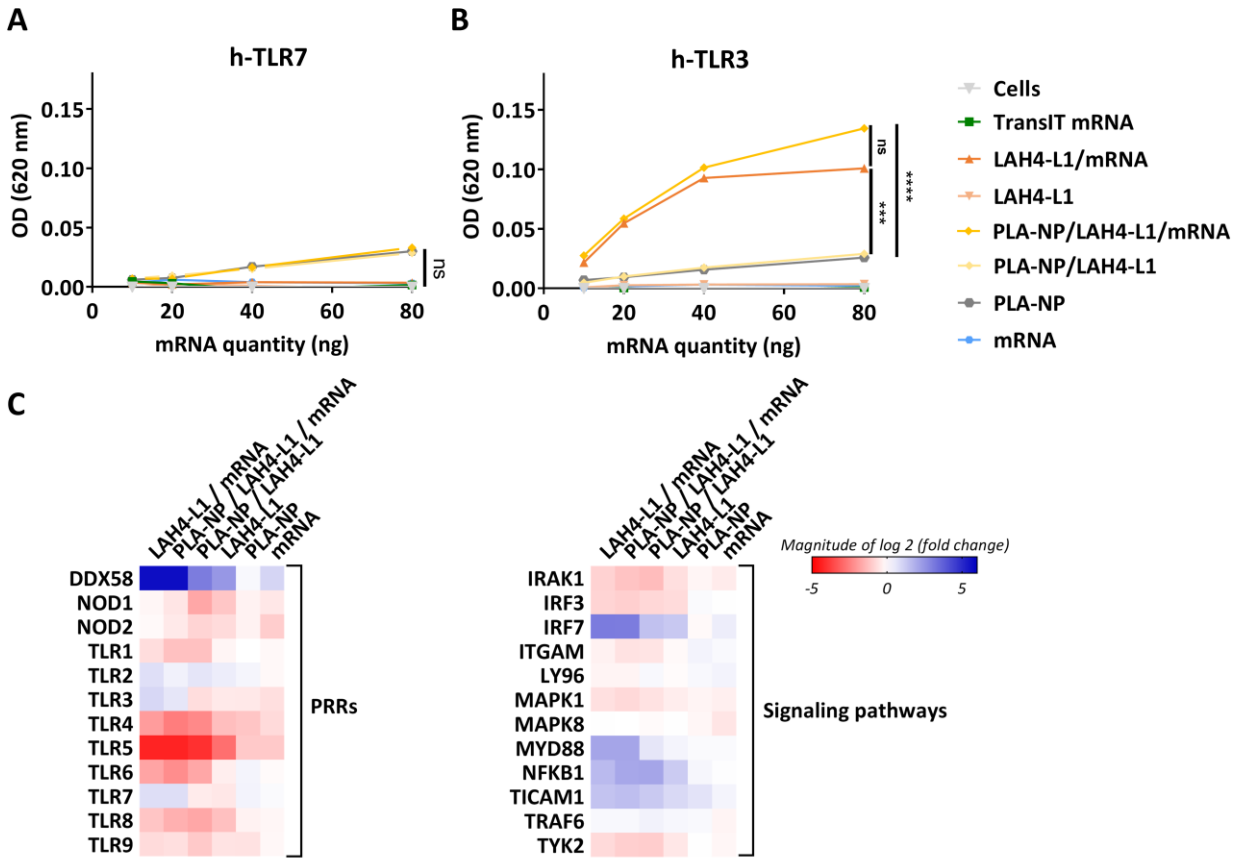

represent a signature of moDCs 6h after transfection.

Fig 5. mRNA complexes stimulate the innate immunity through PRR activation. *(**A-B**) Evaluation of PRR activation via the TLR7 and TLR3 pathways in HEK-Blue hTLR7 and HEK-Blue hTLR3 cells with mRNA formulations (n=2; N=2 and n=2; N=3 for h-TLR7 and h-TLR3 respectively). Statistical significance between two groups was determined using a two-way Anova test: *, $p < 0.05$; **, $p < 0.01$; ***, $p < 0.001$; ****, $p < 0.0001$. (**C**) Expression profile of TLR pathway genes in moDCs after 6 h stimulation with mRNA formulations. This heat map represents the mean of three independent experiments performed with the supernatant of moDCs derived from three different patients, duplicate points being used in each experimental sample.*

a. LAH4-L1/mRNA and PLA-NP/LAH4-L1/mRNA complexes promote moDC maturation

DCs are central effectors of immunity, acting as messengers between the innate and adaptive immune systems. Their stimulation induces their maturation, antigen presentation and the production of cytokines and chemokines leading to the immune response.

In order to evaluate the impact of our formulations on moDC maturation, we first verified the translational efficiency of gag mRNAs in moDCs. As shown in **Fig. S5** moDCs transfected with gag mRNA formulations express the HIV-1 gag protein.

Then, moDCs were stimulated with formulations containing an equal amount of gag mRNAs for 24 h and 48 h, and the expression of different markers of maturation was analyzed by flow cytometry (**Fig. 6A-E'**). LAH4-L1/gag-mRNA and PLA-NP/LAH4-L1/gag-mRNA formulations induced a moDC maturation similar to that observed with a positive control using lipopolysaccharide (LPS). More precisely, these formulations significantly increased MHC-I, MHC-II, CD80 and CD86 expression after 24 h and 48 h of stimulation, in comparison to naked gag mRNAs or formulations devoid of mRNAs. Comparable but less significant results were obtained for the cluster of differentiation CD40. Altogether, these results suggest that mRNA-based formulations promote moDC maturation in our experimental model.

In addition, the expression of 84 genes associated with innate and adaptive immune responses was evaluated in moDCs after 6 h of stimulation with the different formulations. As shown in **Fig. 6F**, LAH4-L1/mRNA and PLA-NP/LAH4-L1/mRNA complexes induced the overexpression of most of the tested genes encoding pro-inflammatory cytokines and chemokines, such as IFN-α, IFN-β, IL-6 and proteins implicated in inflammation, like MX1. This overexpression was induced by LAH4-L1 peptide and amplified by the presence of mRNA. In agreement to the previous expression data, genes involved in DC maturation (CD40, CD80 and CD86) were also overexpressed, validating the precedent results. As represented in the heat map, immune cell chemoattractant factors (CCL5 and CXCL10) and Th1-related genes (IFNG, IL23A, STAT4 and TBX21) were overexpressed whereas Th2-related (IL-10, IL-4, IL5 or Stat6), Th17-related (IL17A, STAT3) and Tregs genes were downregulated or stable. These results indicate that mRNAs complexed in LAH4-L1-based formulations induce an inflammatory response and seem to activate a Th1-biased immune response in moDCs.

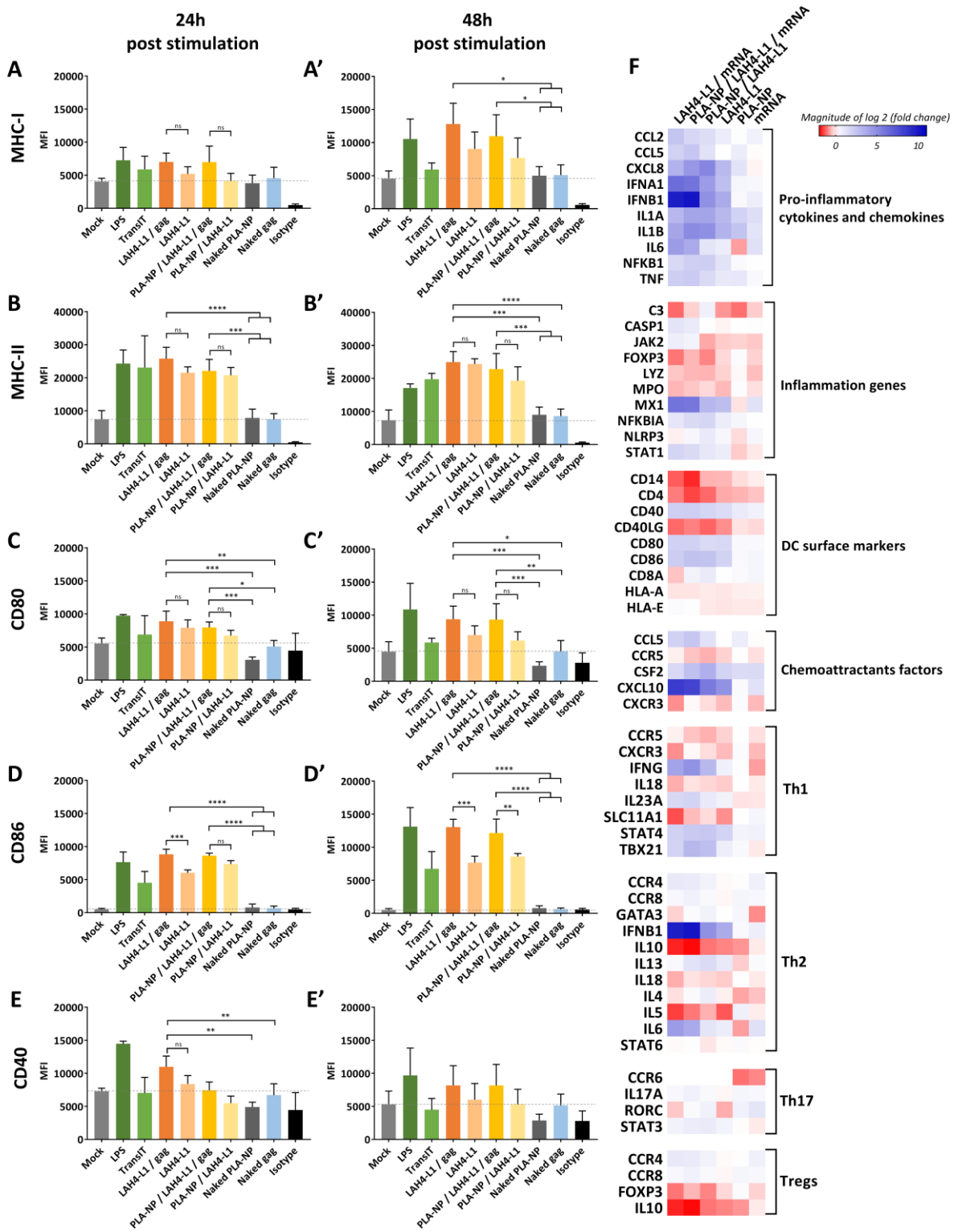

Fig. 6: LAH4-L1/gag-mRNA based formulations induce moDC activation and maturation. *(**A-E'**) Expression of the co-stimulatory molecules MHC-I, MHC-II, CD80, CD86 and CD40 on the surface of CD1a+ CD14– moDCs was determined by flow cytometry 24 h and 48 h after stimulation with volume allowing the transfection of 660 ng of gag mRNA or equivalent volume for controls. The data represent four independent experiments. Statistical significance between two groups was determined using one-way Anova test: *, $p < 0.05$; **, $p < 0.01$; ***, $p < 0.001$, ****, $p < 0.0001$. (**F**) Expression profile of genes iinvolved in innate and adaptive immune response 6 h after stimulation with mRNA formulations (volume allowing the transfection of 2640 ng of gag mRNA or equivalent volume for controls). This heat map represents the mean of three independent experiments performed with the mRNAs of cells from three different patients, duplicate points being used in each experimental sample.*

The maturation of DCs is associated with the expression of cytokines and chemokines that induce and direct adaptive immune responses. The secretion of those mediators implicated in immune response was characterized by Luminex assay 24 h or 48 h after moDC transfection by formulations (**Fig. 7**). Similar profiles were obtained after 24 h and 48 h of stimulation. The presence of gag mRNA in LAH4-L1-based formulations significantly increased the secretion of pro-inflammatory cytokines and chemokines, suggesting a direct impact of mRNA in the inflammatory response. More precisely, LAH4-L1/mRNA formulations induced the secretion of pro-inflammatory cytokines (IL-1α, IL6, IFN-α, TNF-α), chemokines (MIP-1β), Th1-related (IFN-γ, IL-12 (p70)) and Th2-related (IL-13, IL-7) cytokines. However, there was no significant increase in the amount of IL-4 and no secretion of IL-5 (not shown), two well-known markers of the Th2 response. In comparison, PLA-NP/LAH4-L1/mRNA nanocomplexes gave a similar result but with a reduced inflammatory induction (lack of IL-6 and IFN-α) and a higher Th1 induction (IFN-γ, p-value < 0,01; IL-12 (p70), p-value < 0,001).

Overall, these results indicate that LAH4-L1/mRNA and PLA-NP/LAH4-L1/mRNA formulations are potential activators of pro-inflammatory responses and Th1-oriented immune responses, although a subset of Th2-specific markers are also induced.

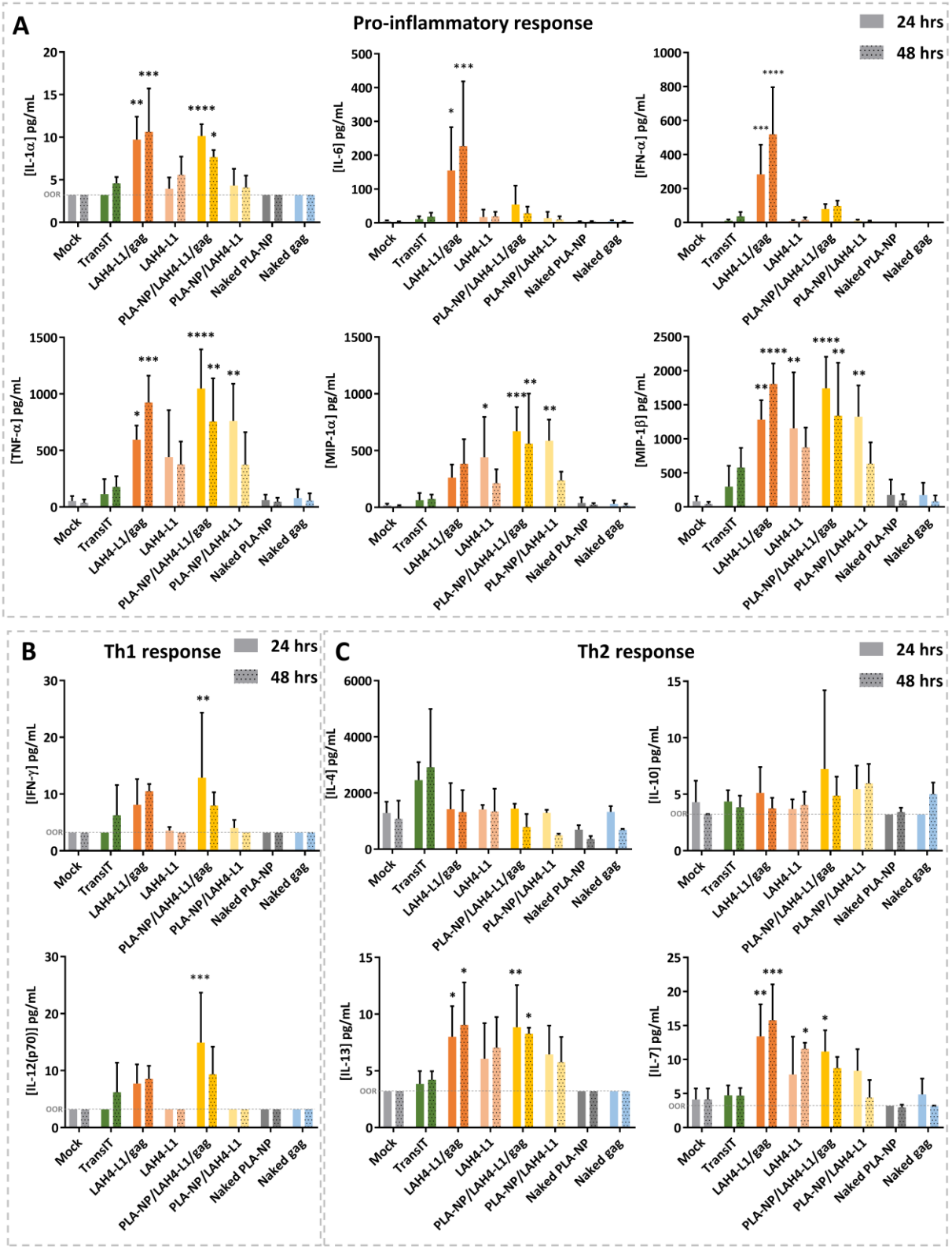

Fig. 7: LAH4-L1/mRNA and PLA-NP/LAH4-L1/mRNA promote cytokine and chemokine secretion by moDCs. *moDCs were stimulated by volume allowing the transfection of 660 ng of gag mRNA or equivalent volume for controls for 24 h or 48 h. The secretion of cytokines and chemokines involved in inflammatory processes (**A**), Th1 (**B**) or Th2 (**C**) immune responses was quantified by Luminex assay on CD1a+ CD14– moDCs supernatants. Data represent the mean of three independents experiments performed with the supernatant of cells from three different patients, triplicate points being used in each experimental sample. OOR; Limit of detection (3.2 pg/mL). Statistical significance between two groups was determined using two-way Anova test: *, $p < 0.05$; **, $p < 0.01$; ***, $p < 0.001$; $p < 0,0001$.*

4. Discussion

In recent years, antigen-encoding mRNAs have emerged as promising alternatives to classical vaccine approaches [9]. The highest challenge with mRNA vaccine is the development of a safe and effective delivery system. Indeed, mRNAs are large polyanionic biomolecules that do not cross efficiently cell membrane barriers in their naked format and are generally unstable in blood circulation, at the site of injection and in the extracellular compartment due to the presence of RNases [45]. While most studies in the mRNA vaccine field have focused on lipid nanoparticles (LNP) [6,9,10,46], we present here a novel platform to vectorize mRNA, using poly(lactic acid) nanoparticles (PLA-NPs) and the amphipathic cationic peptide LAH4-L1, as an intermediate. These formulations allow effective *in vitro* uptake of mRNA by DCs, *via* clathrin-mediated endocytosis and phagocytosis, and efficient mRNA expression, which depends on vacuolar proton ATPase activity and mRNA escape from endosomes. Moreover, these novel mRNA formulations induce DC activation and maturation, and trigger pro-inflammatory and Th1-biased immune responses.

PLA-NPs are versatile biodegradable platform, able to codeliver antigens and/or immunostimulatory molecules to DCs either *in vitro* or *in vivo* [29,30]. However, due to their physicochemical properties, i.e. they are negatively charged, the vectorization of mRNAs using PLA-NPs has been a technological challenge. Thus, we have chosen to use cationic peptides as intermediates. RALA, LAH4 and LAH4-L1 are three cell penetrating peptides (CPPs) with amphipathic cationic properties, which have the ability to condensate nucleic acids [43,47]. However, only few studies have used CPPs to deliver mRNAs [48–50]. In this study, we have developed a strategy based on a two steps process (1) the formation of polyplexes between a cationic peptide and mRNAs and (2) their adsorption onto PLA-NPs (**Fig. 1A**). The three peptides have shown an ability to condensate mRNAs in polyplexes (Peptide/mRNA), which can be adsorbed onto PLA-NPs to form stable nanocomplexes (PLA-NP/Peptide/mRNA) (**Fig. 1B-D and S3**). However, only the LAH4-L1-based formulations have shown promising results for the induction of mRNA expression (**Fig. 2**) and the potentiation of immune responses (**Fig 5-7**). The difference obtained between the three peptides might be partly explained by their structure (**Fig. S1**). Indeed, LAH4-L1, which is a LAH4 derivative, is a histidine-rich, cationic amphipathic peptide with pH-responsive properties. Sequence alignment of these two peptides reveals that two leucine and two histidine residues of LAH4 have been replaced by two histidines and two leucines in LAH4-L1, respectively. According to *in silico* modeling, the new location of the two histidine

residues in the LAH4-L1 peptide narrows the angle subtended by the helix hydrophilic face to 80 degrees, instead of 100 degrees in LAH4. This may give this peptide an enhanced capacity in membrane disruption [43,51].

In this study, we also provided *in vitro* evidence that a low dose of mRNA present in LAH4-L1 and PLA-NP/LAH4-L1-based complexes can induce a strong protein expression in dendritic cells (DCs) (**Fig. 2A-C'**). Moreover, *in vitro* efficiency of mRNA transfection and translation in DCs is significantly more important using these formulations than with TransIT (a commercially reagent) for the same mRNA doses. Although, we found that LAH4- and RALA-based mRNA complexes are unable to transfect DCs, others works have shown efficient transfection of DNA, siRNA and/or recently mRNA transfection using RALA, LAH4 and GALA CPPs in DCs and/or different cell lines [39,43,47,50,52]. These differences may be explained by variations in the experimental conditions, especially regarding the amount of transfected mRNA. Indeed, for RALA-[39] and GALA-[50] based polyplexes, the formulations contain 26- and 10-fold more RNA/cell, respectively, than in our study. Although LAH4-L1- and PLA-NP/LAH4-L1-based formulations were efficient for DC transfection and expression, they failed to induce mRNA expression in HEK293 and HeLa cells (**Fig. 2C and F-G**). Since DCs are specialized in antigen capture and processing [5], the hydrodynamic diameter of LAH4-L1-based complexes might induce DC endocytosis and activation, in comparison to the two epithelial cell lines with a low endocytosis capacities. Hence, a low dose of transfected mRNA could be sufficient to detect its translation in DCs but not in epithelial cells in our assays.

The addition of PLA-NPs to LAH4-L1/mRNA polyplexes induced mRNA expression in a higher number of DCs and at a stronger level (**Fig. 2D and S4**). We showed that in presence of PLA-NPs, the eGFP intensity curve presents a bi-phasic profile with an increase from 4 h to 16-24 h post transfection and a decrease after 24 h (**Fig. 2D**). Using lipid-based formulations to transfect DC lines, Phua *et al*. have shown a biphasic expression kinetics with a rapid peak at 5-7 h, then a rapid decrease of transgene expression until 9 h, followed by gradual loss of expression [53]. Moreover, with a low polydispersity index, nanocomplexes are monodisperse and present a zeta potential of +37,3 mV. Polyplexes present a higher polydispersity index testifying the presence of aggregates and a lower zeta potential (+25,0 mV). Nanocomplexes could force the membrane to bend around the vector and promote its internalization by endocytosis or phagocytosis: this is the wrapping phenomenon described and illustrated by Nel *et al*. [38]. This model implies that the surface charge value, but also the size and shape of the material could directly influence the interaction of the material with

the membranes and thus the uptake of NPs. This could in part explain why nanocomplexes that have a larger surface charge and a more homogeneous size than polyplexes are internalized more efficiently, leading to a more sustained expression in cells. A sustained mRNA expression obtained with PLA-NP/LAH4-L1-based formulations could be advantageous for vaccine applications as it could increase the amount of antigen processed by DCs and consequently immune responses.

Here, we report that LAH4-L1/mRNA and PLA-NP/LAH4-L1/mRNA are taken up by DCs through clathrin-mediated endocytosis and phagocytosis (**Fig. 3**). However, most lipid-based mRNA vaccines are predominantly internalized by micropinocytosis [10,22,54]. It is now well-described that physicochemical properties of delivery systems (such as size, geometry and polydispersity index), but also target cells properties, influence immune recognition and uptake of vaccine by APCs [30,55–57]. The particulate nature and the size of PLA-NP/LAH4-L1/mRNA nanocomplexes, similar to many viruses, could enhance interaction of the vaccine formulations with cell membranes, promoting antigen delivery into cells. LAH4-L1/mRNA polyplexes seem to follow the same internalization mechanisms than PLA-NP/LAH4-L1/mRNA nanocomplexes, which could partly be due to the presence of some aggregates in LAH4-L1/mRNA formulations (**Fig. S2**).

After endocytosis, a pH gradient is established inside the endocytic vesicles, ranging from the least acid early endosomes (pH 6.5 - 6.8) to acidic lysosomes (pH 4.5). mRNAs need to reach the cytosolic compartment to be translated. Protonation of the histidine imidazole groups in LAH4-L1 plays an important role in the transfection process and more importantly for endosomal escape [43]. Indeed, the presence of the pH-responsive cell-penetrating peptide LAH4-L1 in vaccine formulations enhanced mRNA expression in a vacuolar proton ATPase-dependent mechanism (**Fig. 4**), suggesting that LAH4-L1 promoted endosome membrane disruption in DCs for cytosolic delivery of nanocomplexes [58]. Following its release into the cytosol, mRNAs can be translated into antigenic protein. Both endosomal and cytosolic localization of mRNA may participate to their effect on immune responses, as we found that mRNA activates both endosomal (TLR3) and cytosolic (RIG-I) PRRs (**Fig. 4**). mRNAs act as an adjuvant, stimulating the secretion of immune-stimulatory factors. For vaccination, the immune-stimulatory effect and the intrinsic-adjuvant activity of IVT mRNAs could be beneficial, but must be balanced and controlled in time, so that DC activation does not prevent the expression of the antigenic mRNAs supposed to stimulate adaptive immune responses. The activation of both innate and adaptive immune responses is needed for efficient vaccination. The results presented here suggest an ability of LAH4-L1/mRNA and PLA-

NP/LAH4-L1/mRNA nanocomplexes to activate both innate immunity, and a wide spectrum of adaptive immune responses markers (**Fig. 6-7**). The adaptive response signature observed *in vitro* 6 h post transfection suggests that both MHC-I and MHC-II antigen presentation mechanisms are activated, with a prevalent Th1-oriented response and a lower Th2 counterpart (**Fig. 6-7**). This indicates that LAH4-L1/mRNA polyplexes and PLA-NP/LAH4-L1/mRNA nanocomplexes may be suitable mRNA delivery vectors to induce cytotoxic responses in addition to humoral, which remains to be explored *in vivo.* We could observe that gene expression analysis and luminex assays were performed at specific time-points, which can influence some results of specific chemokines. Next step will be to perform the same type of analysis with a more complete kinetic for a longer period of time.

A hypothetical model explaining the different steps leading to cytotoxic and humoral responses after endocytosis of LAH4-L1-gag mRNA-based formulations into DCs is presented in **Fig. 8**. In this scenario, after clathrin-mediated endocytosis or phagocytosis, endosome escape and mRNA translation, the gag protein can be processed and presented through MHC-I allowing T-CD8$^+$ activation and CTL activation. During this period, mRNAs induce the activation of PRRs. The induction of CTLs is potentiated by DC activation and the production of Th1-associated cytokines. Gag expression could also induce vesicles-like particle (VLPs) formation, as described elsewhere [59], which can be later released by DCs and taken up by immature DCs. Secreted VLPs which are recognized like extracellular pathogens, are then processed and presented onto MHC-II, allowing T-CD4$^+$ activation. The generation of an antigen-specific CTL response is important for the development of effective antiviral or antitumor immune responses. Moreover, humoral response is essential to elicit antibodies and memory B cells. The signature of immune responses triggered in primary DCs *in vitro* by LAH4-L1-based gag mRNA formulations, suggests this strategy could be used to transfect human DCs in the case of *ex vivo* therapy, and especially in HIV-1 vaccine-based therapy of chronically infected patients [60,61]. Indeed, by inducing a wide spectrum of both innate and adaptive immune response, this mRNA vaccine formulation would permit clearing the viral reservoir by eliminating infected cells leading to a potential HIV cure[62].

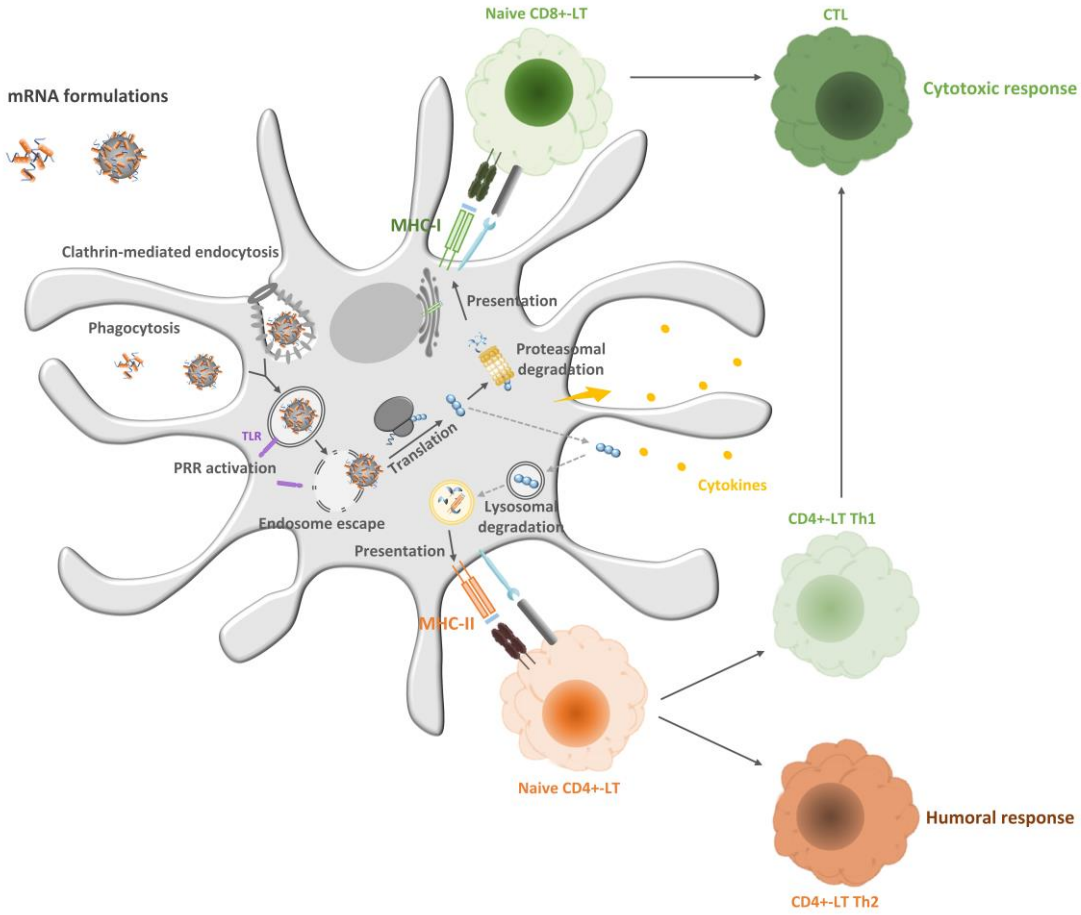

Fig. 8: Model for trafficking of LAH4-L1/mRNA and PLA-NP/LAH4-L1/mRNA into DCs to induce immune responses. *Formulations are taken up by DCs via clathrin-mediated endocytosis or phagocytosis. In the endosomal compartment, LAH4-L1 peptides induce endosome escape and release of mRNA into the cytosol. The presence of mRNA in both endosome and cytosol trigger innate immune stimulation via PRRs. In the cytosol, mRNA is translated into an antigenic protein, which is subsequently processed by the proteasome, and presented onto Major Histocompatibility Complex-type I (MHC-I). This intracellular pathway leads to $CD8^+$ T lymphocyte (LT) activation. Intracellular protein (and especially VLPs formed by gag antigen) can be released by DCs and taken up by novel immature DCs, degraded by lysosomes and presented onto MHC-II. This presentation leads to $CD4^+$ T lymphocyte (LT) activation to form Th1 and Th2 LTs, involed in the activation of cytotoxic and humoral responses, respectively.*

5. Conclusions

In this study, we have designed and developed new strategies to vectorize mRNA using PLA-NPs platform and LAH4-L1 amphipathic cationic peptides. We demonstrated a high capability of LAH4-L1/mRNA and PLA-NP/LAH4-L1/mRNA to transfect DCs and to induce strong protein expression. The presence of PLA-NPs in the formulations enhances this effect. mRNA nanoformulations trigger PRR activation and promote innate immunity activation. Moreover, these complexes could potentiate the humoral immune response, about also a prevalent Th1-biased aspect. Thus, PLA-NP/LAH4-L1/mRNA formulations are

versatile platforms for efficient *in vitro* mRNA delivery to DCs, which could be applied to the *ex vivo* treatment of a wide variety of chronic infectious diseases, like HIV-1.

CONFLICT OF INTEREST

We declare no competing financial interest

AUTHORS CONTRIBUTIONS

ALC participated in the conception and design of the study, performed experiments, analyzed data, and wrote the manuscript. CLG selected peptides and designed formulations. BV participated in the conception and design of the study. JYE, ED and BV assisted in data analysis, and wrote the manuscript. PMG performed uptake analysis and assisted in the moDC purification. CM performed FRET analysis. All the authors read, critiqued, and approved the final manuscript.

ACKNOWLEDGEMENTS

We acknowledge the contribution of SFR Biosciences (UMS3444/CNRS, US8/Inserm, ENS de Lyon, UCBL): AniRA-Cytométrie platform, for assistance with flow cytometry and the PLATIM-Microscopie platform. We also acknowledge Simon Megy for its helps in bioinformatic analysis, and Guido Vanham for pGEM4z-HxB2-gag-64A plasmid and eGFP mRNA and Christophe Guillon for p17 antibody gifts.

FINANCIAL SUPPORT

ALC was supported by a regional fellowship (ARC Santé / Région Auvergne Rhone-Alpes) for three years. Financial support is gained from ANRS in the framework of HIVERA JTC 2014 (HIV-NANOVA) and from ANR-16-CE20-0002-01 (FishRNAVax) to BV, ED and CLG.

REFERENCES

[1] S. Plotkin, History of vaccination, PNAS. 111 (2014) 12283–12287 SPECIAL. doi:10.1073/pnas.1400472111.

[2] C.M.C. Rodrigues, M. V. Pinto, M. Sadarangani, S.A. Plotkin, Whither vaccines?, J. Infect. 74 (2017) S2–S9. doi:10.1016/S0163-4453(17)30184-6.

[3] V. Appay, D.C. Douek, D.A. Price, CD8+ T cell efficacy in vaccination and disease, Nat. Med. 14 (2008) 623–628. doi:10.1038/nm.f.1774.

[4] M. Moser, O. Leo, Key concepts in immunology, Vaccine 28S. 28 (2010) 2–13. doi:10.1016/j.vaccine.2010.07.022.

[5] R.M. Steinman, J. Banchereau, Taking dendritic cells into medicine, Nature. 449 (2007) 419–426. doi:10.1038/nature06175.

[6] A.J. Geall, C.W. Mandl, J.B. Ulmer, RNA: the new revolution in nucleic acid vaccines, Semin. Immunol. 25 (2013) 152–9. doi:10.1016/j.smim.2013.05.001.

[7] U. Sahin, K. Karikó, Ö. Türeci, mRNA-based therapeutics — developing a new class of drugs, Nat. Rev. Drug Discov. 13 (2014) 759–780. doi:10.1038/nrd4278.
[8] S. Pascolo, The messenger's great message for vaccination, Expert Rev. Vaccines. 14 (2015) 153–6. doi:10.1586/14760584.2015.1000871.
[9] N. Pardi, M.J. Hogan, F.W. Porter, D. Weissman, mRNA vaccines - a new era in vaccinology., Nat. Rev. Drug Discov. 17 (2018) 261–279. doi:10.1038/nrd.2017.243.
[10] C. Pollard, S. De Koker, X. Saelens, G. Vanham, J. Grooten, Challenges and advances towards the rational design of mRNA vaccines, Trends Mol. Med. 19 (2013) 705–13. doi:10.1016/j.molmed.2013.09.002.
[11] M. Zhao, M. Li, Z. Zhang, T. Gong, X. Sun, Induction of HIV-1 gag specific immune responses by cationic micelles mediated delivery of gag mRNA, Drug Deliv. 23 (2015) 2596–2607. doi:10.3109/10717544.2015.1038856.
[12] S. Uchida, H. Kinoh, T. Ishii, A. Matsui, T.A. Tockary, K.M. Takeda, H. Uchida, K. Osada, K. Itaka, K. Kataoka, Systemic delivery of messenger RNA for the treatment of pancreatic cancer using polyplex nanomicelles with a cholesterol moiety, Biomaterials. 82 (2016) 221–228. doi:10.1016/J.BIOMATERIALS.2015.12.031.
[13] D. Benteyn, C. Heirman, A. Bonehill, K. Thielemans, K. Breckpot, mRNA-based dendritic cell vaccines, Expert Rev. Vaccines. 14 (2015) 161–176. doi:10.1586/14760584.2014.957684.
[14] H. Debus, P. Baumhof, J. Probst, T. Kissel, Delivery of messenger RNA using poly(ethylene imine)-poly(ethylene glycol)-copolymer blends for polyplex formation: biophysical characterization and in vitro transfection properties, J. Control. Release. 148 (2010) 334–43. doi:10.1016/j.jconrel.2010.09.007.
[15] T. Démoulins, P. Milona, P.C. Englezou, T. Ebensen, K. Schulze, R. Suter, C. Pichon, P. Midoux, C.A. Guzmán, N. Ruggli, K.C. McCullough, Polyethylenimine-based polyplex delivery of self-replicating RNA vaccines, Nanomedicine Nanotechnology, Biol. Med. 12 (2016) 711–722. doi:10.1016/j.nano.2015.11.001.
[16] S. Li, M.A. Rizzo, S. Bhattacharya, L. Huang, Characterization of cationic lipid-protamine-DNA (LPD) complexes for intravenous gene delivery, Gene Ther. 5 (1998) 930–7. doi:10.1038/sj.gt.3300683.
[17] B. Petsch, M. Schnee, A.B. Vogel, E. Lange, B. Hoffmann, D. Voss, T. Schlake, A. Thess, K.-J. Kallen, L. Stitz, T. Kramps, Protective efficacy of in vitro synthesized, specific mRNA vaccines against influenza A virus infection., Nat. Biotechnol. 30 (2012) 1210–6. doi:10.1038/nbt.2436.
[18] T. Bettinger, R.C. Carlisle, M.L. Read, M. Ogris, L.W. Seymour, Peptide-mediated RNA delivery: a novel approach for enhanced transfection of primary and post-mitotic cells, Nucleic Acids Res. 29 (2001) 3882–91. http://www.ncbi.nlm.nih.gov/pubmed/11557821 (accessed August 10, 2018).
[19] F.T. Zohra, E.H. Chowdhury, S. Tada, T. Hoshiba, T. Akaike, Effective delivery with enhanced translational activity synergistically accelerates mRNA-based transfection, Biochem. Biophys. Res. Commun. 358 (2007) 373–378. doi:10.1016/J.BBRC.2007.04.059.
[20] F.T. Zohra, E.H. Chowdhury, T. Akaike, High performance mRNA transfection through carbonate apatite–cationic liposome conjugates, Biomaterials. 30 (2009) 4006–4013. doi:10.1016/j.biomaterials.2009.02.050.
[21] C. Pollard, J. Rejman, W. De Haes, B. Verrier, E. Van Gulck, T. Naessens, S. De Smedt, P. Bogaert, J. Grooten, G. Vanham, S. De Koker, Type I IFN Counteracts the Induction of Antigen-Specific Immune Responses by Lipid-Based Delivery of mRNA Vaccines, Mol. Ther. 21 (2013) 251–259. doi:10.1038/mt.2012.202.
[22] L.M. Kranz, M. Diken, H. Haas, S. Kreiter, C. Loquai, K.C. Reuter, M. Meng, D. Fritz,

F. Vascotto, H. Hefesha, C. Grunwitz, M. Vormehr, Y. Hüsemann, A. Selmi, A.N. Kuhn, J. Buck, E. Derhovanessian, R. Rae, S. Attig, J. Diekmann, R.A. Jabulowsky, S. Heesch, J. Hassel, P. Langguth, S. Grabbe, C. Huber, Ö. Türeci, U. Sahin, Systemic RNA delivery to dendritic cells exploits antiviral defence for cancer immunotherapy, Nature. 534 (2016) 396–401. doi:10.1038/nature18300.

[23] A.J. Geall, A. Verma, G.R. Otten, C.A. Shaw, A. Hekele, K. Banerjee, Y. Cu, C.W. Beard, L.A. Brito, T. Krucker, D.T. O'Hagan, M. Singh, P.W. Mason, N.M. Valiante, P.R. Dormitzer, S.W. Barnett, R. Rappuoli, J.B. Ulmer, C.W. Mandl, Nonviral delivery of self-amplifying RNA vaccines, Proc. Natl. Acad. Sci. U. S. A. 109 (2012) 14604–9. doi:10.1073/pnas.1209367109.

[24] N. Pardi, S. Tuyishime, H. Muramatsu, K. Kariko, B.L. Mui, Y.K. Tam, T.D. Madden, M.J. Hope, D. Weissman, Expression kinetics of nucleoside-modified mRNA delivered in lipid nanoparticles to mice by various routes, J. Control. Release. 217 (2015) 345–351. doi:10.1016/j.jconrel.2015.08.007.

[25] K. Bahl, J.J. Senn, O. Yuzhakov, A. Bulychev, L.A. Brito, K.J. Hassett, M.E. Laska, M. Smith, Ö. Almarsson, J. Thompson, A.M. Ribeiro, M. Watson, T. Zaks, G. Ciaramella, Preclinical and Clinical Demonstration of Immunogenicity by mRNA Vaccines against H10N8 and H7N9 Influenza Viruses, Mol. Ther. 25 (2017) 1316–1327. doi:10.1016/j.ymthe.2017.03.035.

[26] N. Pardi, M.J. Hogan, R.S. Pelc, H. Muramatsu, H. Andersen, C.R. DeMaso, K.A. Dowd, L.L. Sutherland, R.M. Scearce, R. Parks, W. Wagner, A. Granados, J. Greenhouse, M. Walker, E. Willis, J.-S. Yu, C.E. McGee, G.D. Sempowski, B.L. Mui, Y.K. Tam, Y.-J. Huang, D. Vanlandingham, V.M. Holmes, H. Balachandran, S. Sahu, M. Lifton, S. Higgs, S.E. Hensley, T.D. Madden, M.J. Hope, K. Karikó, S. Santra, B.S. Graham, M.G. Lewis, T.C. Pierson, B.F. Haynes, D. Weissman, Zika virus protection by a single low-dose nucleoside-modified mRNA vaccination, Nature. 543 (2017) 248–251. doi:10.1038/nature21428.

[27] J.M. Richner, B.W. Jagger, C. Shan, C.R. Fontes, K.A. Dowd, B. Cao, S. Himansu, E.A. Caine, B.T.D. Nunes, D.B.A. Medeiros, A.E. Muruato, B.M. Foreman, H. Luo, T. Wang, A.D. Barrett, S.C. Weaver, P.F.C. Vasconcelos, S.L. Rossi, G. Ciaramella, I.U. Mysorekar, T.C. Pierson, P.-Y. Shi, M.S. Diamond, Vaccine Mediated Protection Against Zika Virus-Induced Congenital Disease, Cell. 170 (2017) 273–283.e12. doi:10.1016/j.cell.2017.06.040.

[28] V.B. Joshi, S.M. Geary, A.K. Salem, Biodegradable particles as vaccine antigen delivery systems for stimulating cellular immune responses, Hum. Vaccin. Immunother. 9 (2013) 2584–90. doi:10.4161/hv.26136.

[29] V. Pavot, M. Berthet, J. Rességuier, S. Legaz, N. Handké, S.C. Gilbert, S. Paul, B. Verrier, Poly(lactic acid) and poly(lactic- co-glycolic acid) particles as versatile carrier platforms for vaccine delivery, Nanomedicine. 9 (2014) 2703–2718. doi:10.2217/nnm.14.156.

[30] A. Gutjahr, C. Phelip, A.-L. Coolen, C. Monge, A.-S. Boisgard, S. Paul, B. Verrier, Biodegradable Polymeric Nanoparticles-Based Vaccine Adjuvants for Lymph Nodes Targeting., Vaccines. 4 (2016). doi:10.3390/vaccines4040034.

[31] A. Mahapatro, D.K. Singh, Biodegradable nanoparticles are excellent vehicle for site directed in-vivo delivery of drugs and vaccines, J. Nanobiotechnology. 9 (2011) 55. doi:10.1186/1477-3155-9-55.

[32] B. Tyler, D. Gullotti, A. Mangraviti, T. Utsuki, H. Brem, Polylactic acid (PLA) controlled delivery carriers for biomedical applications, Adv. Drug Deliv. Rev. 107 (2016) 163–175. doi:10.1016/j.addr.2016.06.018.

[33] V. Pavot, N. Rochereau, C. Primard, C. Genin, E. Perouzel, T. Lioux, S. Paul, B.

Verrier, Encapsulation of Nod1 and Nod2 receptor ligands into poly(lactic acid) nanoparticles potentiates their immune properties, J. Control. Release. 167 (2013) 60–7. doi:10.1016/j.jconrel.2013.01.015.

[34] A. Gutjahr, L. Papagno, F. Nicoli, A. Lamoureux, F. Vernejoul, T. Lioux, E. Gostick, D.A. Price, G. Tiraby, E. Perouzel, V. Appay, B. Verrier, S. Paul, Cutting Edge: A Dual TLR2 and TLR7 Ligand Induces Highly Potent Humoral and Cell-Mediated Immune Responses, J. Immunol. 198 (2017) 4205–4209. doi:10.4049/jimmunol.1602131.

[35] N. Climent, S. Munier, N. Piqué, F. García, V. Pavot, C. Primard, V. Casanova, J.M. Gatell, B. Verrier, T. Gallart, Loading dendritic cells with PLA-p24 nanoparticles or MVA expressing HIV genes induces HIV-1-specific T cell responses, Vaccine. 32 (2014) 6266–6276. doi:10.1016/j.vaccine.2014.09.010.

[36] C. Primard, N. Rochereau, E. Luciani, C. Genin, T. Delair, S. Paul, B. Verrier, Traffic of poly(lactic acid) nanoparticulate vaccine vehicle from intestinal mucus to sub-epithelial immune competent cells, Biomaterials. 31 (2010) 6060–8. doi:10.1016/j.biomaterials.2010.04.021.

[37] J. Rességuier, E. Delaune, A.-L. Coolen, J.-P. Levraud, P. Boudinot, D. Le Guellec, B. Verrier, Specific and Efficient Uptake of Surfactant-Free Poly(Lactic Acid) Nanovaccine Vehicles by Mucosal Dendritic Cells in Adult Zebrafish after Bath Immersion., Front. Immunol. 8 (2017) 190. doi:10.3389/fimmu.2017.00190.

[38] A.E. Nel, L. Mädler, D. Velegol, T. Xia, E.M. V Hoek, P. Somasundaran, F. Klaessig, V. Castranova, M. Thompson, Understanding biophysicochemical interactions at the nano-bio interface., Nat. Mater. 8 (2009) 543–57. doi:10.1038/nmat2442.

[39] V.K. Udhayakumar, A. De Beuckelaer, J. McCaffrey, C.M. McCrudden, J.L. Kirschman, D. Vanover, L. Van Hoecke, K. Roose, K. Deswarte, B.G. De Geest, S. Lienenklaus, P.J. Santangelo, J. Grooten, H.O. McCarthy, S. De Koker, Arginine-Rich Peptide-Based mRNA Nanocomplexes Efficiently Instigate Cytotoxic T Cell Immunity Dependent on the Amphipathic Organization of the Peptide, Adv. Healthc. Mater. 6 (2017) 1601412. doi:10.1002/adhm.201601412.

[40] Z. Shen, G. Reznikoff, G. Dranoff, K.L. Rock, Cloned dendritic cells can present exogenous antigens on both MHC class I and class II molecules., J. Immunol. 158 (1997) 2723–30. http://www.ncbi.nlm.nih.gov/pubmed/9058806 (accessed August 29, 2018).

[41] S. Legaz, J.-Y. Exposito, C. Lethias, B. Viginier, C. Terzian, B. Verrier, Evaluation of polylactic acid nanoparticles safety using Drosophila model, Nanotoxicology. 10 (2016) 1136–1143. doi:10.1080/17435390.2016.1181806.

[42] J. Rejman, V. Oberle, I.S. Zuhorn, D. Hoekstra, Size-dependent internalization of particles via the pathways of clathrin- and caveolae-mediated endocytosis., Biochem. J. 377 (2004) 159–69. doi:10.1042/BJ20031253.

[43] B. Langlet-Bertin, C. Leborgne, D. Scherman, B. Bechinger, A. James Mason, A. Kichler, Design and Evaluation of Histidine-Rich Amphipathic Peptides for siRNA Delivery, Pharm. Res. 27 (2010) 1426–1436. doi:10.1007/s11095-010-0138-2.

[44] A. Gutjahr, G. Tiraby, E. Perouzel, B. Verrier, S. Paul, Triggering Intracellular Receptors for Vaccine Adjuvantation, Trends Immunol. 37 (2016) 716. doi:10.1016/j.it.2016.08.005.

[45] J.E. Pérez-Ortín, P. Alepuz, S. Chávez, M. Choder, Eukaryotic mRNA Decay: Methodologies, Pathways, and Links to Other Stages of Gene Expression, J. Mol. Biol. 425 (2013) 3750–3775. doi:10.1016/j.jmb.2013.02.029.

[46] P. Midoux, C. Pichon, Lipid-based mRNA vaccine delivery systems, Expert Rev. Vaccines. 14 (2015) 221–234. doi:10.1586/14760584.2015.986104.

[47] H.O. McCarthy, J. McCaffrey, C.M. McCrudden, A. Zholobenko, A.A. Ali, J.W. McBride, A.S. Massey, S. Pentlavalli, K.-H. Chen, G. Cole, S.P. Loughran, N.J. Dunne, R.F. Donnelly, V.L. Kett, T. Robson, Development and characterization of self-assembling nanoparticles using a bio-inspired amphipathic peptide for gene delivery, J. Control. Release. 189 (2014) 141–149. doi:10.1016/j.jconrel.2014.06.048.
[48] G.D. Bell, Y. Yang, E. Leung, G.W. Krissansen, mRNA transfection by a Xentry-protamine cell-penetrating peptide is enhanced by TLR antagonist E6446, PLoS One. 13 (2018) e0201464. doi:10.1371/journal.pone.0201464.
[49] I.R. de Figueiredo, J.M. Freire, L. Flores, A.S. Veiga, M.A.R.B. Castanho, Cell-penetrating peptides: A tool for effective delivery in gene-targeted therapies, IUBMB Life. 66 (2014) 182–194. doi:10.1002/iub.1257.
[50] B. Lou, S. De Koker, C.Y.J. Lau, W.E. Hennink, E. Mastrobattista, mRNA polyplexes with post-conjugated GALA peptides efficiently target, transfect and activate antigen presenting cells, Bioconjug. Chem. (2018). doi:10.1021/acs.bioconjchem.8b00524.
[51] P. Midoux, C. Pichon, J.-J. Yaouanc, P.-A. Jaffrès, Chemical vectors for gene delivery: a current review on polymers, peptides and lipids containing histidine or imidazole as nucleic acids carriers, Br. J. Pharmacol. 157 (2009) 166–78. doi:10.1111/j.1476-5381.2009.00288.x.
[52] R. Bennett, A. Yakkundi, H.D. McKeen, L. McClements, T.J. McKeogh, C.M. McCrudden, K. Arthur, T. Robson, H.O. McCarthy, RALA-mediated delivery of FKBPL nucleic acid therapeutics, Nanomedicine (Lond). 10 (2015) 2989–3001. doi:10.2217/nnm.15.115.
[53] K.K.L. Phua, K.W. Leong, S.K. Nair, Transfection efficiency and transgene expression kinetics of mRNA delivered in naked and nanoparticle format, J. Control. Release. 166 (2013) 227–33. doi:10.1016/j.jconrel.2012.12.029.
[54] S. Persano, M.L. Guevara, Z. Li, J. Mai, M. Ferrari, P.P. Pompa, H. Shen, Lipopolyplex potentiates anti-tumor immunity of mRNA-based vaccination, Biomaterials. 125 (2017) 81–89. doi:10.1016/j.biomaterials.2017.02.019.
[55] V. Manolova, A. Flace, M. Bauer, K. Schwarz, P. Saudan, M.F. Bachmann, Nanoparticles target distinct dendritic cell populations according to their size, Eur. J. Immunol. 38 (2008) 1404–13. doi:10.1002/eji.200737984.
[56] M.F. Bachmann, G.T. Jennings, Vaccine delivery: a matter of size, geometry, kinetics and molecular patterns, Nat. Rev. Immunol. 10 (2010) 787–96. doi:10.1038/nri2868.
[57] K.L. Douglas, C.A. Piccirillo, M. Tabrizian, Cell line-dependent internalization pathways and intracellular trafficking determine transfection efficiency of nanoparticle vectors, Eur. J. Pharm. Biopharm. 68 (2008) 676–687. doi:10.1016/J.EJPB.2007.09.002.
[58] S.M. Farkhani, A. Valizadeh, H. Karami, S. Mohammadi, N. Sohrabi, F. Badrzadeh, Cell penetrating peptides: Efficient vectors for delivery of nanoparticles, nanocarriers, therapeutic and diagnostic molecules, Peptides. 57 (2014) 78–94. doi:10.1016/J.PEPTIDES.2014.04.015.
[59] E.O. Freed, HIV-1 assembly, release and maturation, Nat. Rev. Microbiol. 13 (2015) 484–496. doi:10.1038/nrmicro3490.
[60] L. Leal, C. Lucero, J.M. Gatell, T. Gallart, M. Plana, F. García, New challenges in therapeutic vaccines against HIV infection, Expert Rev. Vaccines. 16 (2017) 587–600. doi:10.1080/14760584.2017.1322513.
[61] L. Leal, A.C. Guardo, S. Morón-López, M. Salgado, B. Mothe, C. Heirman, P. Pannus, G. Vanham, H.J. van den Ham, R. Gruters, A. Andeweg, S. Van Meirvenne, J. Pich, J.A. Arnaiz, J.M. Gatell, C. Brander, K. Thielemans, J. Martínez-Picado, M. Plana, F. García, iHIVARNA consortium, Phase I clinical trial of an intranodally administered

mRNA based therapeutic vaccine against HIV-1 infection, AIDS. (2018) 1. doi:10.1097/QAD.0000000000002026.

[62] B. Autran, Toward a cure for HIV-Seeking effective therapeutic vaccine strategies, Eur. J. Immunol. 45 (2015) 3215–3221. doi:10.1002/eji.201545513.

SUPPLEMENTARY DATA

Table I: Mode of action and working concentration of chemical inhibitor used

Inhibitors	Endocytosis pathways inhibited	Mode of action	Working concentration	Ref
Genistein (Sigma-aldrich)	Caveolae-dependent endocytosis	Inhibits actin cytoskeleton	50 µM	[1,2]
Chlorpromazine (Sigma-aldrich)	Clathrin-mediated endocytosis	Dissociation of clathrin and adaptator from plasma membrane	15 µg/mL	[2]
Dynasore (Sigma-aldrich)	Caveolae and clathrin-dependent endocytosis	Inhibits dynamin	50 µM	[3]
Nocodazole (Sigma-aldrich)	Caveolae and clathrin-dependent endocytosis	Blocks transport from early to late endosomes through inhibition of microtubules polymerization	1.25 µg/mL	[4]
Amiloride (Sigma-aldrich)	Macropinocytosis	Inhibits the Na^+/H^+ exchange protein	100 µM	[2,5]
Pimozide (Sigma-aldrich)	Phagocytosis	Specific Ca^{2+}/calmodulin inhibitor	10 µM	[6]
Cytochalasin D (Sigma-aldrich)	Macropinocytosis and phagocytosis	Potent inhibitor of actin polymerization	10 µM	[2]

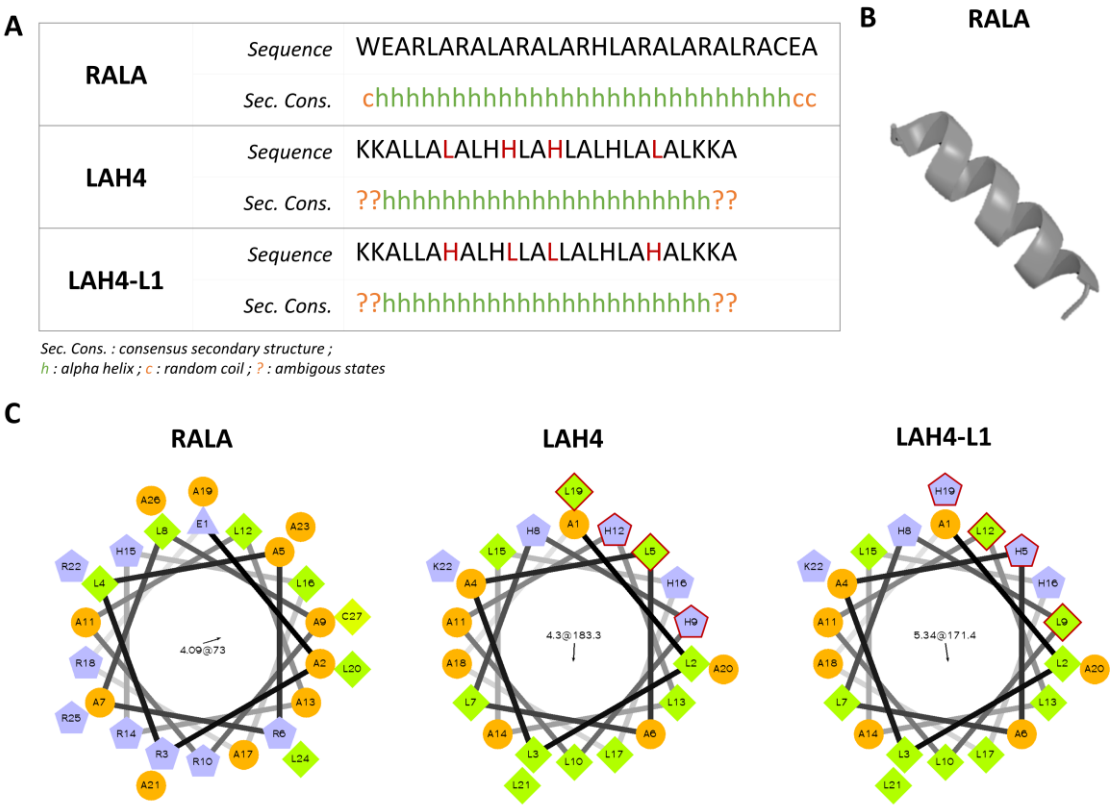

Figure S1: Sequence and predictive structure of RALA, LAH4 and LAH4-L1 peptides. *(**A**) Sequence and secondary structure of RALA, LAH4 and LAH4-L1, based on NPS@ (Network Protein Sequence Analysis) interactive web server using 9 predictions[7]. In green (h) was represented the predicted alpha helix structure and in orange (c) the random coil. Question mark (?) represent ambiguous state. Modified amino acids between LAH4 and LAH4-L1 sequence are red. (**B**) Representation of RALA structure in alpha helix (rzlab.com) (**C**) Helical wheel projection of RALA, LAH4 and LAH4-L1. The output represents the hydrophilic residues as circles, hydrophobic residues as diamonds, potentially negatively charged amino acids as triangles, and potentially positively charged residues as pentagons. Hydrophobicity is color coded as well: hydrophobic residue is green and hydrophilic residues are coded orange. The potentially charged residues are light blue. Modified amino acids between LAH4 and LAH4-L1 sequence are outlined in red.*

A

Nanocomplex	Hydrodynamic diameter (nm)	PdI	Zeta potential (mV)
PLA-NP	188.0 (± 1.80)	0.053 (± 0.046)	- 51.8 (± 0.6)
LAH4-L1 / mRNA	262.0 (± 24.1)	0.300 (± 0.49)	+ 25.0 (± 2.8)
PLA-NP / **LAH4-L1** / mRNA	220.1 (± 22.9)	0.129 (± 0.058)	+ 37.3 (± 4.4)

B

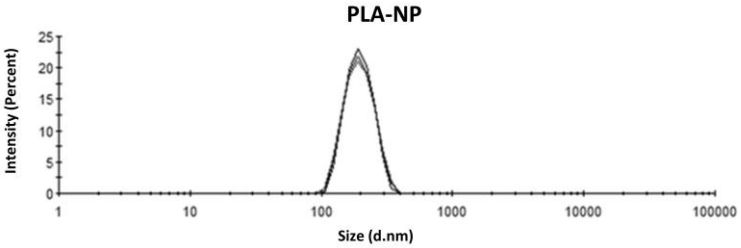

C

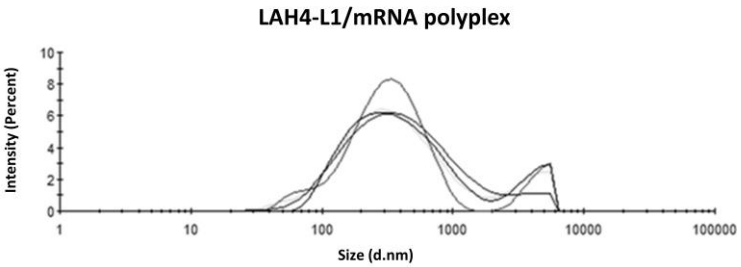

D

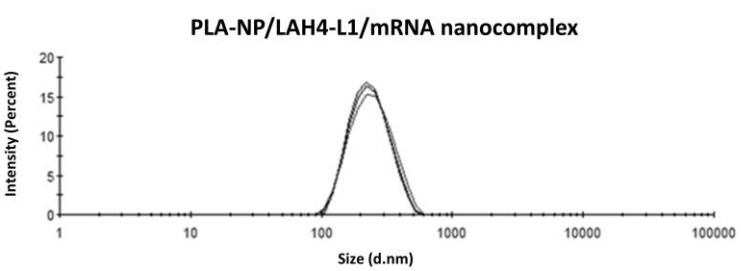

Figure S2: Characterization of LAH4-L1/mRNA and PLA-NP/LAH4-L1/mRNA by DLS. *(**A**) Evaluation of PLA-NP (in grey), LAH4-L1/mRNA (in orange) and PLA-NP/LAH4-L1/mRNA (in yellow) hydrodynamic diameter, polydispersity index (PdI) and zeta potential. Each value provided is the average of four series of measurements in five independent experiments (N=5). (**B**-**D**) Graphs represent the size distribution by intensity of the four measurements obtained in one representative experiment for Naked PLA-NP (B), LAH4-L1/mRNA polyplex (C) and PLA-NP/LAH4-L1/mRNA nanocomplex (D), respectively.*

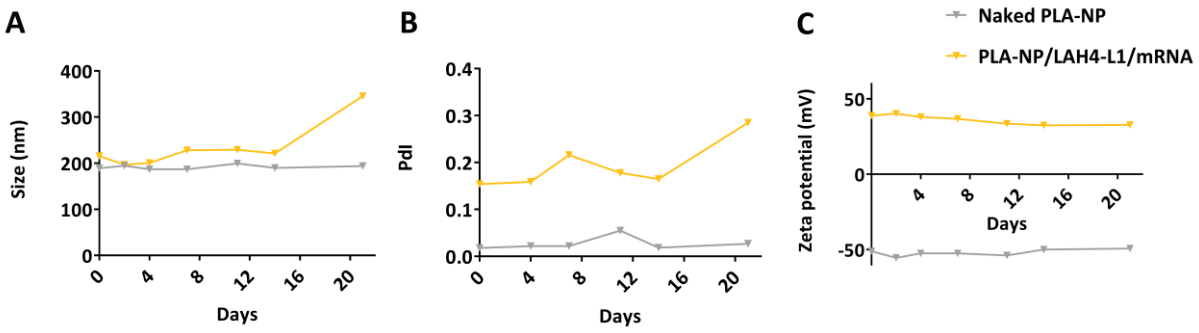

Figure S3: Stability of PLA-NP/LAH4-L1/mRNA formulation at 4°C over 21 days. *Evaluation of PLA-NP (in grey) and PLA-NP/LAH4-L1/mRNA (in yellow) hydrodynamic diameter (**A**), polydispersity index (PdI) (**B**) and surface charge (**C**) over 21 days at 4°C. Each value provided is the average of four series of measurements.*

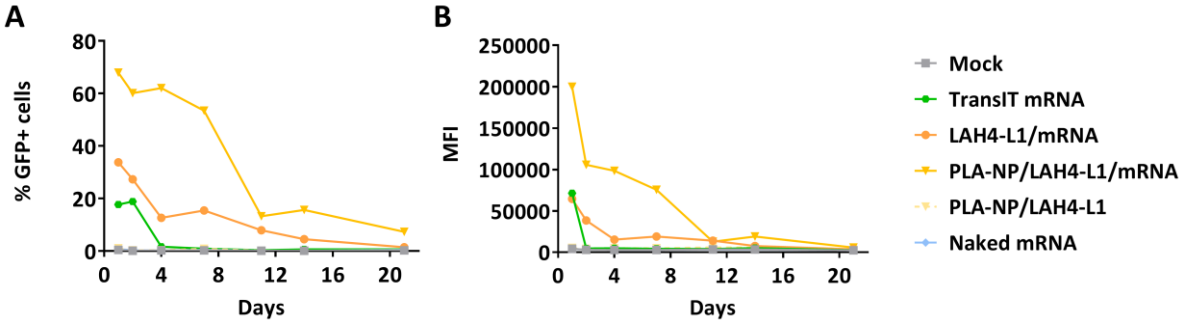

Figure S4: LAH4-L1 formulations retain ability to the induce efficient mRNA expression in DCs after conservation at 4°C for up to 7 days. *Formulations were performed at day 0 and conserved at 4°C during 21 days. At each time point, untreated DCs (Mock), TransIT mRNA (positive control), mRNA complexes and negative controls (PLA-NP/LAH4-L1 and naked mRNA) were transfected in serum-free medium for 4 hours (20 ng mRNA/well), and the transfection efficiency was measured after 16h. (**A**) Percentage of green fluorescent protein (eGFP) positive DC2.4 cells (**B**) mean fluorescence intensity (MFI).*

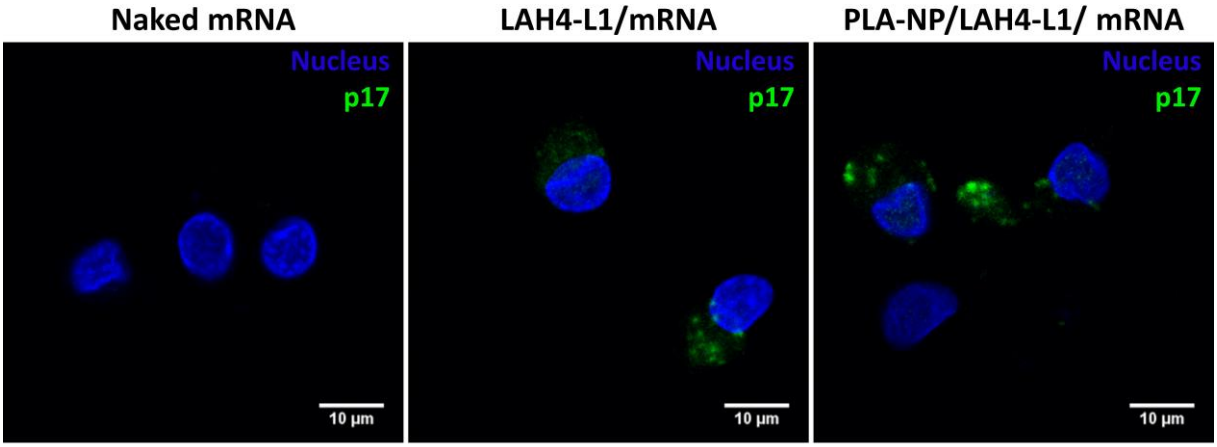

Figure S5: Expression of gag mRNA in moDCs*. Gag mRNAs, either naked or complexed in LAH4-L1-based formulations, were transfected into moDCs in serum-free medium during 4 hours (20 ng mRNA/well). An immunostaining of p17 protein, a component of gag polyprotein, was performed after 16 h. p17 is in green (FITC) and nuclei, in blue (DAPI).*

Supplementary references

[1] L.H. Wang, K.G. Rothberg, R.G. Anderson, Mis-assembly of clathrin lattices on endosomes reveals a regulatory switch for coated pit formation, J. Cell Biol. 123 (1993) 1107–17. http://www.ncbi.nlm.nih.gov/pubmed/8245121.

[2] I.A. Khalil, K. Kogure, H. Akita, H. Harashima, Uptake Pathways and Subsequent Intracellular Trafficking in Nonviral Gene Delivery, Pharmacol. Rev. 58 (2006) 32–45. doi:10.1124/pr.58.1.8.

[3] E. Macia, M. Ehrlich, R. Massol, E. Boucrot, C. Brunner, T. Kirchhausen, Dynasore, a Cell-Permeable Inhibitor of Dynamin, Dev. Cell. 10 (2006) 839–850. doi:10.1016/j.devcel.2006.04.002.

[4] A.I. Idilli, P. Morandini, E. Onelli, S. Rodighiero, M. Caccianiga, A. Moscatelli, Microtubule Depolymerization Affects Endocytosis and Exocytosis in the Tip and Influences Endosome Movement in Tobacco Pollen Tubes, Mol. Plant. 6 (2013) 1109–1130. doi:10.1093/mp/sst099.

[5] J.P. Lim, P.A. Gleeson, Macropinocytosis: an endocytic pathway for internalising large gulps, Immunol. Cell Biol. 89 (2011) 836–843. doi:10.1038/icb.2011.20.

[6] K.A. Key, A.C. Oakley, S. V Pizzo, Effects of pimozide and penfluridol on the binding and endocytosis of alpha 2-macroglobulin-CH3NH2 by mouse peritoneal macrophages, Biochem. Pharmacol. 33 (1984) 3712–4. http://www.ncbi.nlm.nih.gov/pubmed/6210087.

[7] C. Combet, C. Blanchet, C. Geourjon, G. Deléage, NPS@: network protein sequence analysis., Trends Biochem. Sci. 25 (2000) 147–50. doi:https://doi.org/10.1016/S0968-0004(99)01540-6.